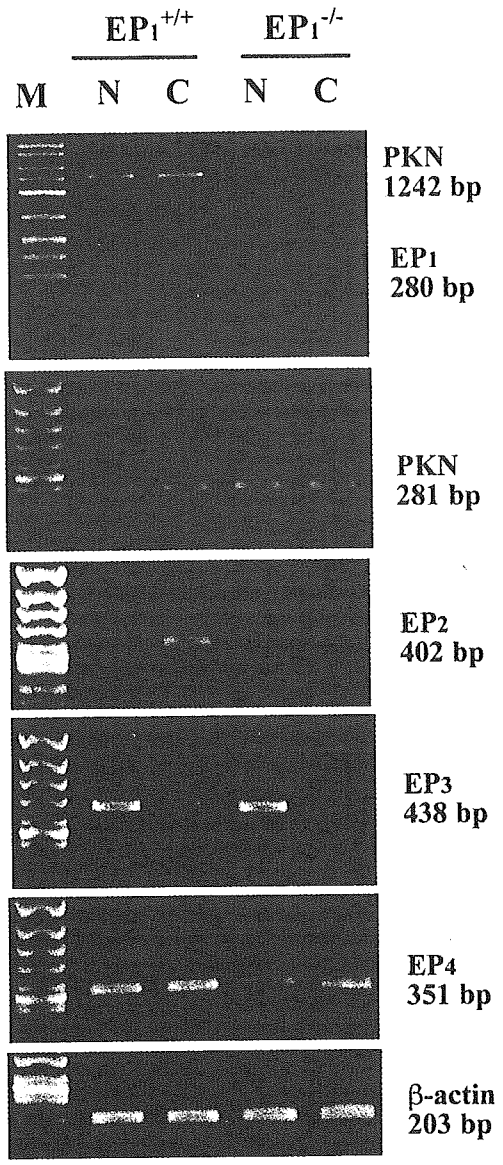

Fig. 3. EP receptors and *PKN* gene expression using RT-PCR. Lanes M, N and C indicate molecular weight control, normal mucosa and cancer of the colon, respectively. The left two lanes represent samples from $EP_1^{+/+}$ mice and the right two lanes represent samples from $EP_1^{-/-}$ mice. (Upper panel) Agarose gel indicating results for EP_1 receptor and *PKN* gene expression using primers *a* and *b*. (Second panel) Agarose gel indicating results for PKN encoding region expression using primers *c* and *d*. (Third, fourth, fifth and sixth panels) Agarose gels indicating results for EP_2, EP_3, EP_4 and β-actin gene expression, respectively.

mRNA for the PKN encoding region was at the same level in the kidneys of all $EP_1^{+/+}$ and $EP_1^{-/-}$ mice (data not shown). These results suggest that the EP_1 knockout strategy and AOM-induced colon carcinogenesis do not affect *PKN* gene stability. Thus, we conclude that colon cancer development was reduced by lack of the EP_1 receptor, not *PKN* gene instability. Next, we examined expression of other *EP* receptor mRNAs in normal mucosa and cancers of the colon in $EP_1^{+/+}$ and $EP_1^{-/-}$ mice (Figure 3, lower panels). The data clearly indicate the EP_2 receptor to be up-regulated and the EP_3 receptor down-regulated in colon cancers. The EP_4 receptor was detected in both normal mucosa and cancers of the colon. There were no differences in the results on EP receptors expression except for EP_1 between $EP_1^{-/-}$ and $EP_1^{+/+}$ mice.

Recently it was reported that the EP_2 receptor is important for intestinal polyp formation in $Apc^{\Delta 716}$ heterozygote mice (30). The authors found analogous results for *EP* receptor mRNA expression using RT-PCR, as in the present study. They, however, indicated no differences in EP_1 receptor expression between polyps and normal mucosa in both small and large intestine. The difference between our and their results may be due to the use of different samples, such as colon adenocarcinomas and intestinal polyps, respectively.

The results of this study clearly show that EP_1 receptor deficiency decreases colon cancer incidence induced by AOM from 57 to 27%. However, 27% of $EP_1^{-/-}$ mice still developed colon cancers. Interestingly, the EP_2 receptor was up-regulated and the EP_3 receptor was down-regulated in colon cancers in $EP_1^{-/-}$ mice. The EP_1 receptor mediates a PGE_2-induced elevation in free Ca^{2+} concentration in Chinese hamster ovary cells and is able to regulate Ca^{2+} channel gating via an as yet unidentified G protein (24). The EP_2 and EP_4 receptors are coupled to G_s and mediate increases in cAMP levels (25). Although alternative splicing of the EP_3 receptor gene results in several isoforms in animal species, including the mouse, rat and human (31–33), the major signaling pathway of the EP_3 receptor is inhibition of adenylate cyclase via G_i. Therefore, there may be cross-talk between second messengers after ligand binding to EP receptors and all four types of EP receptor may interact with each other. Further investigations to identify down stream coordination of these receptors are required.

In conclusion, EP_1 receptor knockout mice demonstrate significantly reduced AOM-induced colon cancer development compared with wild-type mice due to down-regulation of cell proliferation and up-regulation of apoptosis in cancer cells. Also, EP_1 receptor mRNA was found to be up-regulated in colon cancers. These results suggest that the EP_1 receptor plays a pivotal role in colon carcinogenesis and support the hypothesis that lack of the EP_1 receptor has the potential for a mechanism-based chemoprevention strategy against colon cancer development. Therefore, EP_1 receptor antagonists may be a promising chemopreventive agent against colon carcinogenesis. Further studies on the chemopreventive potential of EP_1 receptor antagonists for colon cancer in long-term *in vivo* animal models are ongoing in our laboratory.

Acknowledgements

We thank Ms Yukari Teramoto for her excellent technical support. This work was supported in part by Grants-in-Aid for Cancer Research and the Second-Term Comprehensive 10-Year Strategy for Cancer Research from the Ministry of Health, Labour and Welfare, Japan.

References

1. Thun,M.J., Namboodiri,M.M. and Heath,C.W.,Jr (1991) Aspirin use and reduced risk of fatal colon cancer. *N. Engl. J. Med.*, **325**, 1593–1596.
2. Reddy,B.S., Tokumo,K., Kulkarni,N., Aligia,C. and Kelloff,G. (1992) Inhibition of colon carcinogenesis by prostaglandin synthesis inhibitors and related compounds. *Carcinogenesis*, **13**, 1019–1023.
3. Singh,J., Hamid,R. and Reddy,B.S. (1997) Dietary fat and colon cancer: modulation of cyclooxygenase-2 by types and amount of dietary fat during the postinitiation stage of colon carcinogenesis. *Cancer Res.*, **57**, 3465–3470.
4. Kargman,S.L., O'Neill,G.P., Vickers,P.J., Evans,J.F., Mancini,J.A. and Jothy,S. (1995) Expression of prostaglandin G/H synthase-1 and -2 protein in human colon cancer. *Cancer Res.*, **55**, 2556–2559.
5. Sano,H., Kawahito,Y., Wilder,R.L. *et al.* (1995) Expression of cyclooxygenase-1 and -2 in human colorectal cancer. *Cancer Res.*, **55**, 3785–3789.

6. Kawamori,T., Rao,C.V., Seibert,K. and Reddy,B.S. (1998) Chemopreventive activity of celecoxib, a specific cyclooxygenase-2 inhibitor, against colon carcinogenesis. *Cancer Res.*, **58**, 409–412.
7. Jacoby,R.F., Seibert,K., Cole,C.E., Kelloff,G. and Lubet,R.A. (2000) The cyclooxygenase-2 inhibitor celecoxib is a potent preventive and therapeutic agent in the min mouse model of adenomatous polyposis. *Cancer Res.*, **60**, 5040–5044.
8. Steinbach,G., Lynch,P.M., Phillips,R.K. *et al.* (2000) The effect of celecoxib, a cyclooxygenase-2 inhibitor, in familial adenomatous polyposis. *N. Engl. J. Med.*, **342**, 1946–1952.
9. Tsujii,M. and DuBois,R.N. (1995) Alterations in cellular adhesion and apoptosis in epithelial cells overexpressing prostaglandin endoperoxide synthase 2. *Cell*, **83**, 493–501.
10. Oshima,M., Dinchuk,J.E., Kargman,S.L., Oshima,H., Hancock,B., Kwong,E., Trzaskos,J.M., Evans,J.F. and Taketo,M.M. (1996) Suppression of intestinal polyposis in Apc delta716 knockout mice by inhibition of cyclooxygenase 2 (COX-2). *Cell*, **87**, 803–809.
11. Chulada,P.C., Thompson,M.B., Mahler,J.F. *et al.* (2000) Genetic disruption of Ptgs-1, as well as Ptgs-2, reduces intestinal tumorigenesis in Min mice. *Cancer Res.*, **60**, 4705–4708.
12. Yamaguchi,A., Ishida,T., Nishimura,G., Katoh,M. and Miyazaki,I. (1991) Investigation of colonic prostaglandins in carcinogenesis in the rat colon. *Dis. Colon Rectum*, **34**, 572–576.
13. Rigas,B., Goldman,I.S. and Levine,L. (1993) Altered eicosanoid levels in human colon cancer. *J. Lab. Clin. Med.*, **122**, 518–523.
14. Kawamori,T., Uchiya,N., Sugimura,T. and Wakabayashi,K. (2003) Enhancement of colon carcinogenesis by prostaglandin E2 administration. *Carcinogenesis*, **24**, 985–990.
15. Ushikubi,F., Segi,E., Sugimoto,Y. *et al.* (1998) Impaired febrile response in mice lacking the prostaglandin E receptor subtype EP3. *Nature*, **395**, 281–284.
16. Segi,E., Sugimoto,Y., Yamasaki,A. *et al.* (1998) Patent ductus arteriosus and neonatal death in prostaglandin receptor EP4-deficient mice. *Biochem. Biophys. Res. Commun.*, **246**, 7–12.
17. Hizaki,H., Segi,E., Sugimoto,Y. *et al.* (1999) Abortive expansion of the cumulus and impaired fertility in mice lacking the prostaglandin E receptor subtype EP(2). *Proc. Natl Acad. Sci. USA*, **96**, 10501–10506.
18. Watanabe,K., Kawamori,T., Nakatsugi,S. *et al.* (1999) Role of the prostaglandin E receptor subtype EP1 in colon carcinogenesis. *Cancer Res.*, **59**, 5093–5096.
19. Mutoh,M., Watanabe,K., Kitamura,T. *et al.* (2002) Involvement of prostaglandin E receptor subtype EP(4) in colon carcinogenesis. *Cancer Res.*, **62**, 28–32.
20. Mukai,H. and Ono,Y. (1994) A novel protein kinase with leucine zipper-like sequences: its catalytic domain is highly homologous to that of protein kinase C. *Biochem. Biophys. Res. Commun.*, **199**, 897–904.
21. Batshake,B. and Sundelin,J. (1996) The mouse genes for the EP1 prostanoid receptor and the PKN protein kinase overlap. *Biochem. Biophys. Res. Commun.*, **227**, 70–76.
22. Pozharisski,K.M. (1990) Tumours of the intestines. In Turusov,V. and Mohr,U. (eds) *Pathology of Tumours in Laboratory Animals*, IARC Scientific Publications no. 1. IARC, Lyon, pp. 159–180.
23. Tanaka,T., Takeuchi,T., Nishikawa,A., Takami,T. and Mori,H. (1989) Nucleolar organizer regions in hepatocarcinogenesis induced by N-2-fluorenylacetamide in rats: comparison with bromodeoxyuridine immunohistochemistry. *Jpn. J. Cancer Res.*, **80**, 1047–1051.
24. Watabe,A., Sugimoto,Y., Honda,A., Irie,A., Namba,T., Negishi,M., Ito,S., Narumiya,S. and Ichikawa,A. (1993) Cloning and expression of cDNA for a mouse EP1 subtype of prostaglandin E receptor. *J. Biol. Chem.*, **268**, 20175–20178.
25. Katsuyama,M., Nishigaki,N., Sugimoto,Y., Morimoto,K., Negishi,M., Narumiya,S. and Ichikawa,A. (1995) The mouse prostaglandin E receptor EP2 subtype: cloning, expression and northern blot analysis. *FEBS Lett.*, **372**, 151–156.
26. Sugimoto,Y., Negishi,M., Hayashi,Y., Namba,T., Honda,A., Watabe,A., Hirata,M., Narumiya,S. and Ichikawa,A. (1993) Two isoforms of the EP3 receptor with different carboxyl-terminal domains. Identical ligand binding properties and different coupling properties with Gi proteins. *J. Biol. Chem.*, **268**, 2712–2718.
27. Honda,A., Sugimoto,Y., Namba,T., Watabe,A., Irie,A., Negishi,M., Narumiya,S. and Ichikawa,A. (1993) Cloning and expression of a cDNA for mouse prostaglandin E receptor EP2 subtype. *J. Biol. Chem.*, **268**, 7759–7762.
28. Egan,M.J. and Crocker,J. (1992) Nucleolar organiser regions in pathology. *Br. J. Cancer*, **65**, 1–7.
29. Ruschoff,J., Bittinger,A., Neumann,K. and Schmitz-Moormann,P. (1990) Prognostic significance of nucleolar organizing regions (NORs) in carcinomas of the sigmoid colon and rectum. *Pathol. Res. Pract.*, **186**, 85–91.
30. Sonoshita,M., Takaku,K., Sasaki,N., Sugimoto,Y., Ushikubi,F., Narumiya,S., Oshima,M. and Taketo,M.M. (2001) Acceleration of intestinal polyposis through prostaglandin receptor EP2 in Apc (Delta 716) knockout mice. *Nature Med.*, **7**, 1048–1051.
31. Kotani,M., Tanaka,I., Ogawa,Y., Usui,T., Tamura,N., Mori,K., Narumiya,S., Yoshimi,T. and Nakao,K. (1997) Structural organization of the human prostaglandin EP3 receptor subtype gene (PTGER3). *Genomics*, **40**, 425–434.
32. Namba,T., Sugimoto,Y., Negishi,M., Irie,A., Ushikubi,F., Kakizuka,A., Ito,S., Ichikawa,A. and Narumiya,S. (1993) Alternative splicing of C-terminal tail of prostaglandin E receptor subtype EP3 determines G-protein specificity. *Nature*, **365**, 166–170.
33. Negishi,M., Sugimoto,Y., Irie,A., Narumiya,S. and Ichikawa,A. (1993) Two isoforms of prostaglandin E receptor EP3 subtype. Different COOH-terminal domains determine sensitivity to agonist-induced desensitization. *J. Biol. Chem.*, **268**, 9517–9521.

Received May 26, 2004; revised October 11, 2004; accepted October 19, 2004

Chem. Res. Toxicol. **2005,** *18,* 1553−1562

Structures and Biological Properties of DNA Adducts Derived from *N*-Nitroso Bile Acid Conjugates

Yukari Totsuka,*,† Rena Nishigaki,† Shigeki Enomoto,† Takeji Takamura-Enya,† Ken-ichi Masumura,‡ Takehiko Nohmi,‡ Nobuo Kawahara,‡ Takashi Sugimura,† and Keiji Wakabayashi†

Cancer Prevention Basic Research Project, National Cancer Center Research Institute, 1-1 Tsukiji 5-chome, Chuo-ku, Tokyo 104-0045, Japan, and National Institute of Health Sciences, 1-18-1 Kamiyoga, Setagaya-ku, Tokyo 158-0098, Japan

Received June 3, 2005

A kind of *N*-nitrosobile acid conjugate, *N*-nitrosotaurocholic acid (NO-TCA), was incubated with calf thymus DNA, and formation of an adduct was detected by the ^{32}P-postlabeling method under nuclease P1 conditions. To examine the nucleotides containing the adduct from NO-TCA, each of 2′-deoxyribonucleotide 3′-monophosphates (3′-dAp, 3′-dGp, 3′-dCp, or 3′-Tp) was incubated with NO-TCA. The same adduct spot was detected in the reaction of NO-TCA with 3′-dCp. The structure of this adduct was determined to be 3-ethanesulfonic acid-dC by several spectrometry techniques. Moreover, bulky adducts containing bile acid moiety were also produced from the reaction of NO-TCA with 3′-dCp and 3′-dAp. From comparison with spectral data for authentic compounds, these adducts were concluded to be N^4-cholyl-dC and N^6-cholyl-dA. N^4-Cholyl-dC and N^6-cholyl-dA were also detected in calf thymus DNA treated with NO-TCA. In addition, 3-ethanesulfonic acid-dC and N^4-deoxycholyl-dC were found to be produced from *N*-nitrosotaurodeoxycholic acid (NO-TDCA) with dC. NO-TCA and NO-TDCA induced mutations in *Salmonella typhimurium* TA100 but not in TA98. Mutational spectrum analysis revealed that NO-TCA induced G to A transitions predominantly. When NO-TCA (250 mg/kg) was singly administered to male Wistar rats by gavage, both ethanesulfonic acid-dC and N^4-cholyl-dC could be detected in the glandular stomach and colon. The levels of ethanesulfonic acid-dC were 0.22−0.29 per 10^6 nucleotides, but values for N^4-cholyl-dC were about 500-fold lower. These observations suggest that *N*-nitroso bile acid conjugates, NO-TCA and NO-TDCA, may induce G to A base substitutions in genes via DNA adduct formation, producing ethanesulfonic acid- and/or (deoxy)cholic acid-DNA and, therefore, may be related to human carcinogenesis as endogenous mutagens.

Introduction

Epidemiological studies have indicated an association between bile acids and colorectal cancer (*1*, *2*), and high levels of secondary bile acids are present in the feces of populations at high risk of colorectal cancer (*3*, *4*). It has further been reported that deoxycholic acid (DCA)[1] stimulates proliferation of colonic epithelium in vitro and in vivo (*5*, *6*) and suppresses not only spontaneous but also butyrate-induced apoptosis in human colonic adenoma cells in vitro (*7*). In addition, bile acids or bile acid conjugates, such as cholic acid (CA), chenodeoxycholic acid (CDCA), litocholic acid (LCA), and taurodeoxycholic acid (TDCA), promote development of colorectal adenomas and adenocarcinomas in rats (*8*, *9*). There is some evidence of formation of DNA adducts with bile acids in vitro (*10*−*13*).

N-Nitroso bile acid conjugates, such as *N*-nitrosoglycocholic acid (NO-GCA) and *N*-nitrosotaurocholic acid (NO-TCA), have already been demonstrated to exert mutagenic activity in both bacterial and mammalian assay systems (*14*, *15*). Moreover, these compounds also can induce liver and stomach cancers in F344 rats (*16*). *N*-Nitroso bile acid conjugates are also thought to be among the presumed carcinogens of stomach and esophageal tumor development in rat duodenogastoric reflux models (*17*−*19*). For this purpose, rats are subjected to surgery in order to induce duodenal reflux into the stomach or the esophagus, thus being chronically exposed to the mixture of duodenal and gastric juice. After 50 weeks of such exposure, adenocarcinomas are found in the digestive tract without exogenous carcinogens, at reported incidences of 31−41% for stomach and 44% for esophagus. In general, patients undergoing distal gastrectomy have been reported to be at increased risk of gastric carcinoma (*20*, *21*). It has been shown that the risk is higher after Billroth II rather than Billroth I resection (*20*, *22*, *23*), the difference reflecting levels of duodenogastric reflux. The amounts of bile acid conjugates in humans are reported to be 16−40 mg/mL in bile juice, 0.08−6.77 mg/mL in gastric juices from patients

* To whom correspondence should be addressed. Tel: +81-3-3547-5201(ext. 4353). Fax: +80-3-3543-9305. E-mail: ytotsuka@gan2.res.ncc.go.jp.
† National Cancer Center Research Institute.
‡ National Institute of Health Sciences.

[1] Abbreviations: DCA, deoxycholic acid; CA, cholic acid; CDCA, chenodeoxycholic acid; LCA, litocholic acid; NO-GCA, *N*-nitrosoglycocholic acid; NO-TCA, *N*-nitrosotaurocholic acid; NO-TDCA, *N*-nitrosotaurodeoxycholic acid; 3′-dAp, 2′-deoxyadenosine 3′-monophosphate; 3′-dGp, 2′-deoxyguanosine 3′-monophosphate; 3′-dCp, 2′-deoxycitidine 3′-monophosphate; 3′-Tp, thymidine 3′-monophosphate; dA, 2′-deoxyadenosine; dG, 2′-deoxyguanosine; dC, 2′-deoxycitidine; dT, 2′-deoxytymidine; N^4-cholyl-dC, N^4-cholyl-2′-deoxycytidine; N^6-cholyl-dA, N^6-cholyl-2′-deoxyadenosine; PEI, polyethyleneimine; T4-PNK, T4-polynucleotide kinase.

10.1021/tx050144x CCC: $30.25
Published on Web 09/14/2005

with bile reflux gastritis, and 0.29−3.45 μg/mL in serum (*24*, *25*). Because intragastric formation of nitrosamides could be mediated by acid-catalyzed reaction of amides with nitrite, *N*-nitroso compounds have been suggested as plausible etiological factors in development of gastric cancer in humans (*26*, *27*). In fact, it has also been reported that taurocholic acid (TCA) is nitrosated in simulated gastric juice (*14*). Moreover, thioproline, an effective nitrite-trapping agent, could inhibit the development of esophageal adenocarcinoma induced by gastroduodenal reflux in rats (*19*). Such nitrosation is also suggested to be mediated by activated macrophages in infected and inflamed organs. Therefore, it is likely that nitrosated bile acid conjugates could contribute to cancer development as endogenous mutagens.

It is reported that O^6-carboxymethyl-guanine, 7-carboxymethyl-guanine, and 3-carboxymethyl-adenine are produced in vitro when *N*-nitrosoglycocholic acid (NO-GCA) is incubated with calf thymus DNA under neutral conditions (*28*). Similarly, it is suggested that *N*-nitrosotauroursodeoxycholic acid would form ethane sulfonic acid-DNA; however, the structure is not fully known yet (*27*). Moreover, little is known about the formation of bulky adducts containing bile acid moieties; we recently found that bile acid-DNA adducts could be formed by the reaction of DNA with cholyl adenylate, a reactive intermediate in the production of bile acid-amino acid conjugates. Structural analyses determined these bile acid-DNA adducts to be N^4-cholyl-2′-deoxycytidine (N^4-cholyl-dC) and N^6-cholyl-2′-deoxyadenosine (N^6-cholyl-dA) (*29*). Therefore, it is possible that similar bile acid-DNA adducts might be formed from *N*-nitroso bile acid conjugates. In the present study, we investigated the formation and chemical structures of DNA adducts containing ethane sulfonic acid and bile acid moieties, produced by the reaction of *N*-nitroso bile acid conjugates, NO-TCA, and *N*-nitrosotaurodeoxycholic acid (NO-TDCA), with DNA. Moreover, mutagenic activities of *N*-nitroso bile acid conjugates and their mutation spectra in *Salmonella typhimurium* TA100 were also examined. We also report here the formation of DNA adducts in some tissues of rats administered NO-TCA. From these results, the biological significance of NO-TCA and NO-TDCA as endogenous mutagens is discussed.

Materials and Methods

Materials. NO-TCA and NO-TDCA were obtained from the Nard Institute (Osaka, Japan). 2′-Deoxyribonucleotide 3′-monophosphate (3′-dAp, 3′-dGp, 3′-dCp, and 3′-Tp) and 2′-deoxyribonucleoside (dA, dG, dC, and T) were from Sigma Chemical Co. (St. Louis, MO). Micrococcal nuclease and phosphodiesterase II were purchased from Worthington Biochemical Co. (Freehold, NJ). [γ-^{32}P]ATP, T4 polynucleotidekinase (T4-PNK), nuclease P1, and phosphodiesterase I were obtained from ICN Biochemicals (Irvine, CA), Takara Shuzo Co. (Kyoto, Japan), Yamasa Shoyu Co. (Choshi, Japan), and Worthington Biochemical Co., respectively. All other chemicals used were of analytical grade.

Spectral Measurements. ^{1}H NMR spectra were recorded with JEOLGX-α600 or α800 instruments using microprobe FT-NMR spectrometers. Electronspray ionization mass spectrometry (ESI-MS) was performed using a Waters ZQ 2000 mass spectrometer equipped with an Agilent 1100 HPLC system. UV absorbance spectra were measured on a PD-8020 photodiode array detector (Tosoh, Tokyo, Japan).

Chemical Synthesis of N^4-Cholyl-dC and N^6-Cholyl-dA. Authentic N^4-cholyl-dC and N^6-cholyl-dA were synthesized according to the procedure reported previously (*29*). Briefly, 3′,5′-bis-*O*-*tert*-butyldimethylsilyl-2′-deoxycitiydine (0.1 mmol) or 3′,5′-bis-*O*-*tert*-butyldimethylsilyl-2′-deoxyadenosine (0.1 mmol) was stirred with CA (0.1 mmol) and dicyclohexylcarbodiimide (0.12 mmol) in pyridine at 70 °C for 4 h. The organic phase was evaporated, and then, these residues were separated on column chromatography, followed by deprotection.

Reaction of *N*-Nitrosobile Acid Conjugates and Nucleotide and/or DNA. Ten micromole aliquots of each *N*-nitrosobile acid conjugate (NO-TCA or NO-TDCA) were incubated with 650 nmol of calf thymus DNA in 1 mL of 100 mM phosphate buffer (pH 7.4) at 37 °C for 24 h. Then, DNA was extracted with phenol/chloroform:isoamyl alcohol (24:1 v/v) and precipitated with ethanol. DNA concentrations were measured spectrophotometrically at 260 nm and adjusted to 2 mg/mL in 0.01× SSC buffer. With reactions between *N*-nitrosobile acid conjugates and mononucleotides, 650 nmol of each 2′-deoxyribonucleotide 3′-monophosphate (3′-dAp, 3′-dGp, 3′-dCp, and 3′-Tp) was used instead of calf thymus DNA. Adduct formation was analyzed by the ^{32}P-postlabeling method under nuclease P1 conditions as described below.

Structural Analysis of Ethane Sulfonic Acid-dC Adducts. NO-TCA or NO-TDCA was incubated with dC in 100 mM phosphate buffer (pH 7.4) at 37 °C for 24 h, and the resulting solution was separated by HPLC as follows. An aliquot of the solution was applied to a semipreparative Capcell pack C18 column (5 μm particle size, 10 mm × 250 mm; Shiseido, Tokyo, Japan), and a mobile phase of 2% acetonitrile in 0.25% triethylamine-acetic acid (pH 6.3) was pumped in isocratically at a flow rate of 3 mL/min. In addition to a few peaks detected in the solution without dC, a peak, eluting at a retention time of 9.3 min, was newly observed in the reaction mixture of NO-TCA and dC. The peak was collected and injected into an analytical grade TSKgel ODS-80Ts column (5 μm particle size, 4.6 mm × 250 mm; Tosoh) for further purification. The applied material was eluted at a flow rate of 1 mL/min with a gradient system of 2.5% methanol in 0.1% heptafluorobutylic acid (pH 3.0) for 10 min and then a linear gradient to 80% methanol in 0.1% heptafluorobutylic acid. All of the above HPLC procedures were performed several times at an ambient temperature with monitoring of eluate at 254 nm. The compound was collected for determination of UV absorption, mass, and ^{1}H and ^{13}C NMR spectra. ^{1}H and ^{13}C NMR spectrum assignment of the adduct was performed with DQF-COSY, HMQC, and HMBC. The following data were obtained.

^{1}H NMR (DMSO-d_6): δ 8.09 [d, J = 7.2, H-6 (dC), 1H], 6.11 [d, J = 7.2, H-5 (dC), 1H], 6.07 [t, J = 6.4, H-1′ (dR), 1H], 5.29 [d, J = 4.0, H-3′-OH (dR), 1H], 5.07 [t, J = 4.8, H-5′-OH (dR), 1H], 4.21−4.19 [m, H-3′ (dR), 1H], 4.15 (dd, J = 7.2, 6.4, H-$\underline{CH_2}CH_2SO_3H$, 2H), 3.83 [dd, J = 7.2, 3.2, H-4′ (dR), 1H], 3.61−3.59 [m, H-5″ (dR), 1H], 3.57−3.54 [m, H-5′ (dR), 1H], 2.86 (t, J = 6.4, H-$CH_2\underline{CH_2}SO_3H$, 2H), 2.23−2.21 [m, H-2″ (dR), 1H], 2.13−2.10 [m, H-2′ (dR), 1H]. ^{13}C NMR (DMSO-d_6) δ 159.1 [C-4 (dC)], 147.6 [C-2 (dC)], 140.6 [C-6 (dC)], 95.2 [C-5 (dC)], 88.0 [C-4′ (dR)], 86.6 [C-1′ (dR)], 69.6 [C-3′ (dR)], 60.7 [C-5′ (dR)], 47.1 (C-$CH_2\underline{CH_2}SO_3H$), 41.1 (C-$\underline{CH_2}CH_2SO_3H$). ESI-MS *m/z* 334, 218. UV λ_{max} 219, 280 nm.

Structural Analysis of CA-dC Adducts. NO-TCA was incubated with dC, and the solution was subjected to HPLC under the following conditions. An aliquot was applied to an analytical grade TSKgel ODS-80Ts column (5 μm particle size, 4.6 mm × 250 mm; Tosoh) and eluted at a flow rate of 1 mL/min with a linear gradient of acetonitrile (from 20 to 80%) in 0.1% diethylamine-acetic acid (pH 6.0) over 30 min. In addition to a few peaks detected in the solution without dC, a peak, eluted at a retention time of 21.3 min, was observed in the reaction mixture of NO-TCA and dC. UV absorption and mass spectra showed absorption maxima at 245 and 298 nm and molecular ion peaks at *m/z* 502 and 618. From comparison with the UV and mass spectra for authentic N^4-cholyl-dC, the compound at a peak of 21.3 min was suggested to be a CA-dC adduct. The peak fraction was therefore collected and applied to ^{1}H NMR spectral analyses. The following data were obtained.

^{1}H NMR (DMSO-d_6): δ 10.81 (s, 1H, NHCO), 8.30 [d, J = 7.2, 1H, H-6 (dC)], 7.21 [d, J = 7.2, 1H, H-5 (dC)], 6.09 [t, J = 6.4, 1H, H-1′ (dR)], 5.27 [brs, 1H, 3′-OH (dR)], 5.04 [brs, 1H, 5′-OH (dR)], 4.31 [s, 1H, 3-OH (CA)], 4.20 [brs, 1H, H-3′ (dR)], 4.11 [d, J = 3.2, 1H, 12-OH (CA)], 4.00 [d, J = 3.2, 1H, 7-OH (CA)], 3.84 [dd, J = 7.2, 3.6, 1H, H-4′ (dR)], 3.77 [d, J = 2.8, 1H, H-12 (CA)], 3.60−3.54 [m, 3H, H-7 (CA), H-5′, 5″ (dR)], 3.50−3.17 [m, 1H, H-3 (CA) overlapped with the absorbance signal of H_2O], 2.30−2.13 [m, 5H, H-4α, 9, 23α, 23β (CA), H-2′ (dR)], 2.01−1.98 [m, 2H, H-14 (CA), H-2″ (dR)], 1.79−1.62 [m, 7H, H-17, 20, 22α, 16α, 1α, 6β, 15β (CA)], 1.45−1.14 [m, 12H, H-2α, 2β, 4β, 5, 6α, 8, 11α, 11β, 15α, 16β, 22β (CA)], 0.98−0.92 [m, 4H, H-1β, CH_3-21 (CA)], 0.80 [s, 3H, CH_3-19 (CA)], 0.57 [s, 3H, CH_3-18 (CA)]. ESI-MS *m/z* 618, 502. UV λ_{max} 245, 298 nm.

Structural Analysis of CA-dA Adducts. NO-TCA was incubated with dA as described above and separated by HPLC under the same conditions as for structural analysis of CA-dC adducts. A peak eluting at a retention time of 15.4 min was observed in the reaction mixture, and the UV absorption pattern showed absorption maximum at 273 nm. Because the HPLC eluting position and UV spectrum of the compound were similar to those of the authentic N^6-cholyl-dA, this compound was deduced to be a CA-dA adduct. LC-ESI/MS analysis demonstrated this compound to exhibit a molecular ion at *m/z* 642 and fragment at *m/z* 526, the latter deriving from loss of deoxyribose. Therefore, the chemical structure of the compound was concluded to be N^6-cholyl-dA.

Structural Analysis of DCA-dC Adducts. NO-TDCA and dC were incubated in 100 mM phosphate buffer (pH 7.4) at 37 °C for 24 h and separated by HPLC according to the same procedure as for CA-dC or dA adducts. A peak showing a similar UV absorption pattern to N^4-cholyl-dC was observed at a retention time of 23.0 min and collected for UV, mass, and ^{1}H and ^{13}C NMR spectral analyses. ^{1}H and ^{13}C NMR spectrum assignment of the adduct was conducted with DQF-COSY, HMQC, and HMBC. The following data were obtained.

^{1}H NMR (DMSO-d_6): δ 10.81 (s, 1H, NHCO), 8.30 [d, J = 7.2, 1H, H-6 (dC)], 7.20 [d, J = 7.2, 1H, H-5 (dC)], 6.09 [t, J = 6.2, 1H, H-1′ (dR)], 5.27 [brs, 1H, 3′-OH (dR)], 5.04 [brs, 1H, 5′-OH (dR)], 4.45 [s, 1H, 3-OH (DCA)], 4.20 [brs, 1H, H-3′ (dR)], 3.84 [dd, J = 6.6, 2.4, 1H, H-4′ (dR)], 3.77 [brs, 1H, H-12 (DCA)], 3.59−3.56 [m, 3H, H-7 (DCA), H-5′, 5″ (dR)], 3.50−3.17 [m, 1H, H-3 (DCA)], 2.40−2.25 [m, 5H, H-4α, 9, 23α, 23β (DCA), H-2′ (dR)], 2.02−1.96 [m, 2H, H-14 (DCA), H-2″ (dR)], 1.80−1.44 [m, 8H, H-17, 20, 22α, 16α, 1α, 6β, 7β, 15β (DCA)], 1.35−1.15 [m, 13H, H-2α, 2β, 4β, 5, 6α, 7α, 8, 11α, 11β, 15α, 16β, 22β (DCA)], 1.09−0.91 [m, 4H, H-1β, CH_3-21 (DCA)], 0.83 [s, 3H, CH_3-19 (DCA)], 0.58 [s, 3H, CH_3-18 (DCA)]. ^{13}C NMR (DMSO-d_6): δ 175.0 [C=O (DCA)], 162.9 [C-4 (dC)], 155.0 [C-2 (dC, C=O)], 145.5 [C-6 (dC)], 95.8 [C-5 (dC)], 88.5 [C-4′ (dR)], 86.7 [C-1′ (dR)], 71.6 [C-12 (DCA)], 70.5 [C-3 (DCA), C-3′ (dR)], 61.5 [C-5′ (dR)], 47.4 [C-14 (DCA)], 46.3 [C-17 (DCA)], 46.0 [C-13 (DCA)], 41.6 [C-5 (DCA)], 40.9 [C-2′ (dR)], 40−39 [C-4, 8 (DCA) overlapped with absorbance signal of DMSO], 36.3 [C-23 (DCA)], 35.1 [C-1 (DCA)], 35.0 [C-20 (DCA)], 33.8 [C-10 (DCA)], 32.9 [C-9 (DCA)], 30.9 [C-22 (DCA)], 30.2 [C-2 (DCA)], 28.6 [C-11 (DCA)], 27.1 [C-16 (DCA)], 27.0 [C-6 (DCA)], 26.1 [C-7 (DCA)], 23.5 [C-15 (DCA)], 23.1 [C-19 (DCA)], 17.0 [C-21 (DCA)], 12.5 [C-18 (DCA)]. ESI-MS *m/z* 602, 486. UV λ_{max} 246, 298 nm.

Analysis of DNA Adducts Derived from Bile Acid Conjugates in the Organs of Rats Administered NO-TCA. Five male Wistar rats, purchased from Charles River Japan, Inc. (Atsugi, Japan), were provided with food (CE-2 pellet diet, CLEA Japan) and tap water ad libitum. NO-TCA was dissolved in water and administered to three rats as a single oral dose by gavage at level of 250 mg per kg body wt. The two rats in the control group received the solvent alone. At 24 h after administration of NO-TCA, both chemically treated and control groups of rats were euthanized under ether anesthesia. The major organs, such as the liver, glandular stomach, and colon mucosa, were excised and stored at −80 °C until DNA extraction by a standard procedure with enzymatic digestion of protein and RNA followed by extraction with phenol and chloroform/isoamyl alcohol (24:1, v/v). The experiments were conducted according to the Guidelines for Animal Experiments in National Cancer Center of the Committee for Ethics of Animal Experimentation of the National Cancer Center.

Enzymatic digests of 100 μg aliquots of DNA were subjected to HPLC using the heptafulorobutylic acid-methanol system as described in the structure analysis of 3-ethane sulfonic acid-dC, and the eluents were collected at retention times of 3−4 min for analysis of 3-ethanesulfonic acid-dC and 46−47 min for analysis of N^4-cholyl-dC. The retention times for 3-ethanesulfonic acid-3′-dCp and N^4-cholyl-3′-dCp were confirmed using LC-ESI/MS analysis. After lyophilization of the fractioned samples, residues were dissolved in 10 μL of distilled water and then subjected to ^{32}P-postlabeling analysis under nuclease P1 conditions, as described below.

^{32}P-Postlabeling Method. DNA obtained from the in vitro experiments using calf thymus DNA or the in vivo experiments was digested with micrococcal nuclease and phosphodiesterase II and then ^{32}P-postlabeled using the nuclease P1 enrichment method as reported previously (*30*). For the in vitro experiments using deoxyribonucleotide 3′-monophosphate as a DNA source, ^{32}P-postlabeling was performed under nuclease P1 conditions without DNA digestion.

For the separation of ethanesulfonic acid-DNA adduct, the resulting ^{32}P-postlabeled samples were applied to a polyethyleneimine (PEI) cellulose TLC sheet (POLYGRAM CEL 300 PEI; Macherey-Nagel, Duren, Germany), attached to 10 cm filter paper at the top, and developed with 0.1 M lithium chloride, 3 M acetic acid, and 3 M urea to remove [^{32}P]phosphate and [γ-^{32}P]ATP, as previously reported (*31*).

For the analysis of CA-DNA adducts, the ^{32}P-postlabeled samples were applied to a PEI-cellulose sheet, attached to 10 cm filter paper at the top, and developed with 2.3 M sodium phosphate buffer (pH 6.0) to remove normal nucleotides. The modified nucleotides remaining at the origin were contact-transferred to another PEI-cellulose sheet and then subjected to two-dimensional TLC. The solvent system for development consisted of buffer A (2.07 M lithium formate and 7.65 M urea, pH 3.5) from bottom to top and buffer B (0.90 M lithium chloride, 0.45 M Tris-HCl, and 7.65 M urea, pH 8.0) from left to right, followed by 1.7 M sodium phosphate buffer, pH 6.0, from left to right, with 3.5 cm filter paper.

Adducts were detected with a Bio-Image Analyzer (BAS 2000; Fuji Photo Film Co., Tokyo, Japan) after exposing the TLC sheets to Fuji imaging plates or autoradiography on Kodak XAR-5 film with intensifying screens. Relative adduct labeling was determined by the methods of Gupta et al. (*32*) and Reddy et al. (*30*), and values were calculated as averages using data from three assays.

Mutagenicity Assay. The preincubation method (*33*) was carried out for testing the mutagenicity of *N*-nitrosobile acid conjugates to *S. typhimurium* TA98 and TA100. Briefly, bacterial cells were incubated with the test chemical without S9 mix for 20 min at 37 °C in a total volume of 0.7 mL. The mixture was poured onto agar plates with 2 mL of soft agar and incubated for 2 days at 37 °C. The numbers of His$^+$ revertants per plate were then determined.

Sequencing of *hisG46* Mutations. A 201 bp DNA fragment containing the *hisG46* site was amplified by colony PCR (forward primer: 5′-GAT TGA TAT CCT GCG CGT GCG TG-3′; reverse primer: 5′-TCG TCA ACC GGT GTT GCC AGC G-3′). DNA sequencing was performed with a BigDye Terminater Cycle Sequencing Kit (Applied Biosystems, Foster City, CA) on an ABI PRISM 310 Genetic Analyzer (Applied Biosystems).

Results

Formation of Ethane Sulfonic Acid-dC Adduct by NO-TCA. In reactions of NO-GCA with DNA, 7-carboxymethylguanine and O^6-methylguanine are reported

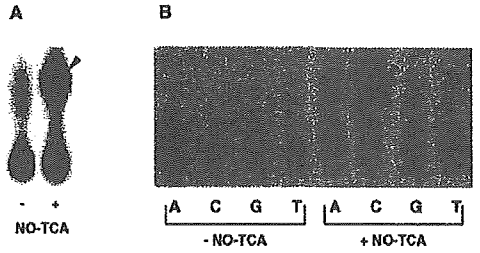

Figure 1. Autoradiogram of ethanesulfonic acid-DNA adducts derived from NO-TCA. Calf thymus DNA (A) or each of 2′-deoxyribonucleotide 3′-monophosphate (B) was incubated with or without NO-TCA, and DNA adduct formation was analyzed by ^{32}P-postlabeling under nuclease P1 conditions. The adduct spots are indicated by the arrowheads.

to be produced, thus taurine-modified DNA adduct is expected to be formed from NO-TCA (*27*, *28*). Therefore, NO-TCA was incubated with 650 nmol of calf thymus DNA under neutral conditions at 37 °C for 24 h and adduct formation was analyzed by ^{32}P-postlabeling under nuclease P1 conditions. TLC development was carried out with 0.1 M lithium chloride, 3 M acetic acid, and 3 M urea, as previously reported, being different from the TLC development systems for bulky adduct (*30*). As shown in Figure 1A, radioactive spots were detected at the origin in the mixture without NO-TCA, but one spot, in an upper position from the origin, was clearly observed in the reaction mixture of NO-TCA and calf thymus DNA. The adduct level was estimated to be 30.2 ± 6.21 per 10^6 nucleotides. To examine the nucleotides involved in the adducts with NO-TCA treatment, the compound was incubated with separate 2′-deoxyribonucleotide 3′-monophosphate (3′-dAp, 3′-dGp, 3′-dCp, and 3′-dTp), and adduct formation was analyzed. As shown in Figure 1B, the same adduct was also detected in the reaction of NO-TCA with 3′-dCp.

To analyze its chemical structure, NO-TCA was incubated with dC and the resulting solution was separated by HPLC. An aliquot of the solution was applied to a semipreparative ODS column, and a peak, eluting at a retention time of 9.3 min, was observed. This peak fraction was then further purified using an analytical grade ODS column, and a peak eluting at a retention time of 9.5 min was collected for analyses of UV absorption, mass, and ^{1}H and ^{13}C NMR spectra. The yield of this adduct from dC was about 1%. Its UV/vis absorption spectrum showed absorption maxima at 280 nm (Figure 2), and mass spectrum analysis revealed a molecular ion at *m/z* 334 corresponding to a protonated derivative of the conjugated product of ethanesulfonic acid and deoxycytidine and a fragmentation ion at *m/z* 218, consistent with loss of the deoxyribose moiety. Figure 3 shows the ^{1}H NMR spectrum of ethanesulfonic acid-dC compound measured in DMSO-d_6. The 15 protons were assigned with DQF-COSY, HMQC, and HMBC. The proton signals corresponding to the 2′-deoxycytidine moiety [H-1′, 2′, 2″, 3′, 4′, 5′, 5″, 3′-OH, 5′-OH (dR), H-5, -6 (dC)] were observed from 2.10 to 8.09 ppm. Moreover, proton signals at 4.15 and 2.86 ppm were assigned to the ethanesulfonic acid moiety. Although no proton signal was observed corresponding to the exocyclic amino group, the N4 position of the cytidine, HMBC analysis showed the signal at 4.15 ppm on ^{1}H NMR spectroscopy of the ethanesulfonic acid moiety to clearly correlate with signal peaks at 159.1 and 147.6 ppm in the ^{13}C NMR spectrum

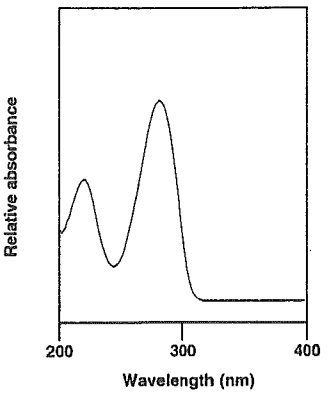

Figure 2. UV/vis absorption spectrum of the ethansulfonic acid-dC adduct. An aliquot of the reaction mixture of NO-TCA and dC was applied to HPLC on an analytical ODS column with a linear gradient of methanol (from 2.5 to 80%) in 0.1% heptafluorobutylic acid (pH 3.0), and the UV/vis absorption spectrum of the ethanesulfonic acid-dC was measured with a photodiode array detector.

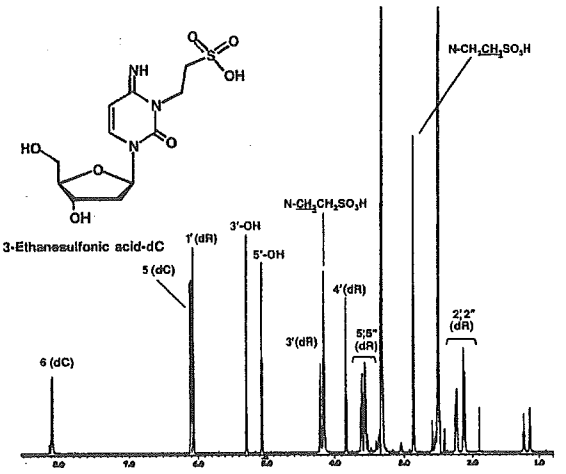

Figure 3. ^{1}H NMR spectrum in DMSO-d_6 and chemical structure of the ethanesulfonic acid-dC adduct.

of the cytidine moiety (see Supporting Information). Therefore, the structure of this compound was concluded to be 3-ethanesulfonic acid-dC (Figure 3).

Formation of CA-dC and -dA Adducts by NO-TCA. As mentioned above, the DNA adduct-containing taurine moiety was clearly formed by NO-TCA. Then, the formation of bile acid-DNA adduct was analyzed by the ^{32}P-postlabeling method, under the different condition from the case of 3-ethanesulfonic acid-dC adduct.

As shown in Figure 4, two major adduct spots (Figure 4A) were clearly detected on reaction of NO-TCA with calf thymus DNA. Levels of these adduct spots were estimated to be 3.40 ± 0.16 (Figure 4A, spot 1) and 1.69 ± 0.20 (Figure 4A, spot 2) per 10^8 nucleotides. In addition, one minor adduct spot (Figure 4A, spot 3) was also observed and the adduct level was almost 10 times lower than those of major spots.

To confirm the nucleotides involved in these adducts, this nitroso compound was incubated with 2′-deoxyribonucleotide 3′-monophosphates, and adduct formation was analyzed by the ^{32}P-postlabeling method under nuclease P1 conditions. As shown in Figure 4B, the major adduct

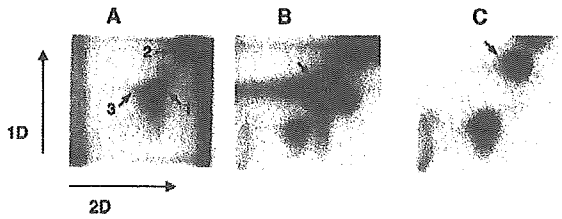

Figure 4. Autoradiograms of bile acid-DNA adducts derived from NO-TCA. NO-TCA was incubated with calf thymus DNA (A), 3′-dCp (B), and 3′-dAp (C) in 100 mM phosphate buffer (pH 7.4) at 37 °C for 24 h. Then adduct formations were analyzed by the ^{32}P-postlabeling method and developed with different conditions from the case of ethanesulfonic acid-dC adduct described in the Materials and Methods. Adducts are indicated by arrows.

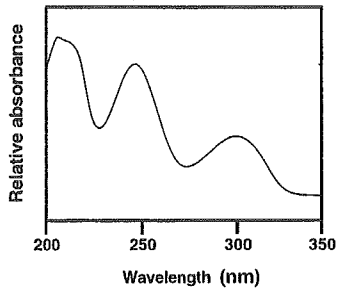

Figure 5. UV/vis absorption spectrum of the CA-dC adduct eluting at a retention time of 21.3 min on an ODS column and measured with a photodiode array detector.

spot (Figure 4A, spot 1) observed with the calf thymus DNA corresponded to the dC adduct, and another spot (Figure 4A, spot 2) corresponded to adduct spot detected in the reaction mixture of NO-TCA and 3′-dAp (Figure 4C). Moreover, the minor adduct spot (Figure 4A, spot 3) was deduced to be a dG adduct (data not shown). From these findings, DNA adducts detected in the NO-TCA treated calf thymus DNA were concluded to be NO-TCA-dC, NO-TCA-dA, and NO-TCA-dG. To analyze the chemical structure of the major adduct, NO-TCA was incubated with dC and the adduct was isolated by HPLC on an ODS column using a linear gradient of an acetonitrile in diethylamine-acetic acid (pH 6.0) solvent system. A peak eluting at a retention time of 21.3 min was observed in the reaction mixture of NO-TCA and dC. Thus, this peak fraction was collected and the UV/vis absorption spectrum of the responsible compound was measured. As shown in Figure 5, its absorption maxima were at 245 and 298 nm. Mass spectrometry demonstrated a molecular ion at *m/z* 618, which corresponded to a protonation product of a CA and deoxycytidine conjugate. A prominent fragment peak observed at *m/z* 502 was consistent with loss of the deoxyribose moiety from the protonated molecule. The authentic sample of N^4-cholyl-dC showed UV absorption maxima at 243 and 295 nm and exhibited a molecular ion of *m/z* 618. Therefore, the dC adduct formed from NO-TCA was deduced to be CA-dC adduct. By repeating the HPLC fractionation, about 400 μg of the CA-dC adduct could be collected for measurement of the ^{1}H NMR spectrum. The yield of CA-dC adduct from dC was about 0.06%. Figure 6A shows the ^{1}H NMR spectrum for the CA-dC adduct measured in DMSO-d_6, indicating the presence of 52 protons, which were assigned by two-dimensional NMR and comparison with NMR spectral data obtained from the authentic sample of N^4-cholyl-dC (Figure 6B). Forty upfield peaks from 0.57 to 4.27 ppm were assigned to the CA moiety. Proton signals corresponding to the 2′-deoxycytidine moiety [H-1′, 2′, 2″, 3′, 4′, 5′, 5″, 3′-OH, 5′-OH (dR), H-5, -6 (dC)] were also observed from 1.98 to 8.30 ppm. Thus, all proton signals of the product formed from NO-TCA and dC agreed with those of authentic N^4-cholyl-dC. Its structure is shown in Figure 7.

From the results of ^{32}P-postlabeling analysis, another major DNA adduct produced by NO-TCA with calf thymus DNA was suggested to contain a dA moiety. Speculating from the results of the dC adduct described above, the structure of the dA adduct derived from NO-TCA was suggested to be N^6-cholyl-dA. To confirm the structure of the NO-TCA-dA adduct, NO-TCA was incubated with dA in 100 mM phosphate buffer (pH 7.4) at 37 °C for 24 h and separated by HPLC under the same conditions for structural analysis of the CA-dC adduct. A peak eluting at a retention time of 15.4 min, the same as for authentic N^6-cholyl-dA, was observed in the reaction mixture. Moreover, this peak fraction had a similar UV absorption spectrum, with an absorption maximum at 273 nm, to that of the authentic sample of N^6-cholyl-dA (absorption maximum at 272 nm). LC-ESI/MS analysis revealed a molecular ion at *m/z* 642, corresponding to a protonated product of a CA and deoxyadenosine conjugate, and a fragmention ion at *m/z* 526, derived from the loss of the deoxyribose moiety from the original compound (Figure 8). From these observations, the chemical structure of this compound was concluded to be N^6-cholyl-2′-dA (Figure 8).

Structures of Adducts Formed by NO-TDCA. The other *N*-nitroso bile acid conjugate, NO-TDCA, would be expected to form similar dC adducts, including ethane sulfonic acid or deoxycholyc acid moiety. Therefore, NO-TDCA was incubated with dC, and the adduct formation was analyzed by LC-ESI/MS. A peak revealing a molecular ion at *m/z* 334 and its fragmentation ion at *m/z* 218 was eluted at the same retention time of 3-ethanesulfonic acid-dC (data not shown). Moreover, the UV/vis absorption pattern of this compound was identical to that of 3-ethanesulfonic acid-dC. Thus, 3-ethanesulfonic acid-dC was also produced from NO-TDCA and dC, and its yield was about the same levels as those of NO-TCA.

To confirm the formation of dC adduct including DCA moiety, NO-TDCA was incubated with dC and the adduct was isolated by HPLC on an ODS column according to the same procedures of N^4-cholyl-dC. The UV absorption pattern of this purified compound was similar to that of N^4-cholyl-dC, and its absorption maxima were at 246 and 298 nm (see Supporting Information). Like the N^4-cholyl-dC adduct, this compound exhibited a molecular ion at *m/z* 602, corresponding to a protonated product of DCA and dC conjugate, and a fragmentation ion at *m/z* 486, consistent with loss of the deoxyribose moiety from the protonated molecule (see Supporting Information). By repeating the HPLC procedures, around 1000 μg of the DCA-dC adduct could be collected for ^{1}H and ^{13}C NMR spectrum analysis. The yield of DCA-dC adduct from dC was 0.02%, and the ^{1}H and ^{13}C NMR spectra were assigned with DQF-COSY, HMQC, and HMBC (see Supporting Information). On the basis of the UV/vis, mass, and NMR spectral data, the structure of the adduct formed from NO-TDCA and dC was concluded to be N^4-deoxycholyl-dC (see Supporting Information).

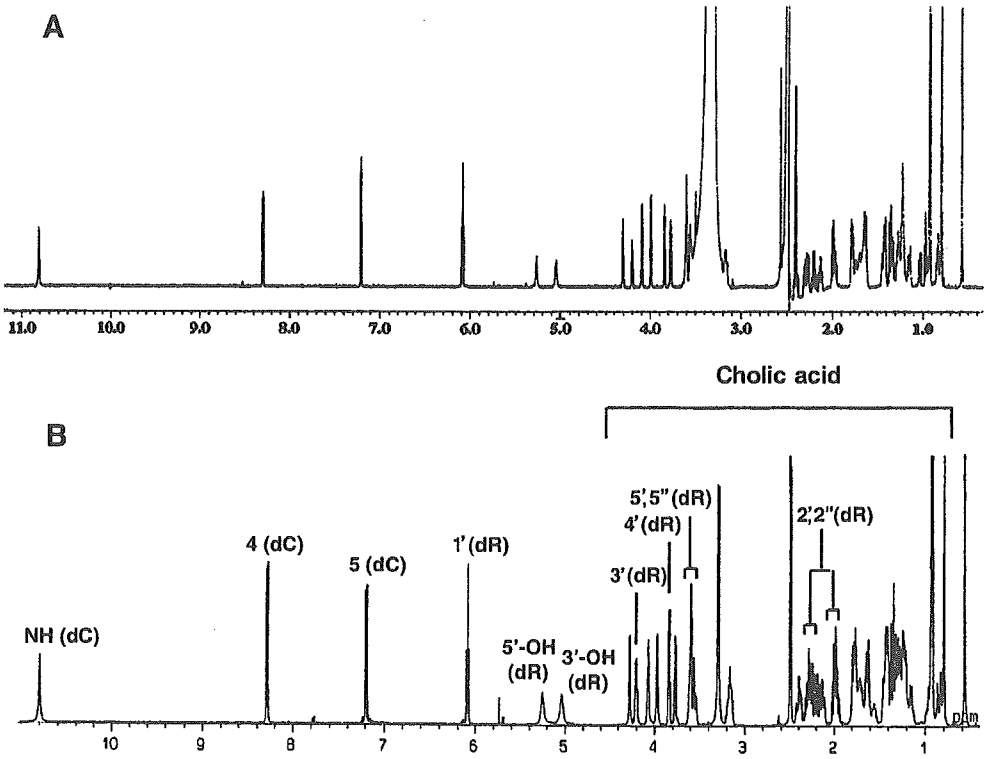

Figure 6. Comparison of the ^{1}H NMR spectra in DMSO-d_6 of CA-dC adduct (A) and authentic N^4-cholyl-dC (B).

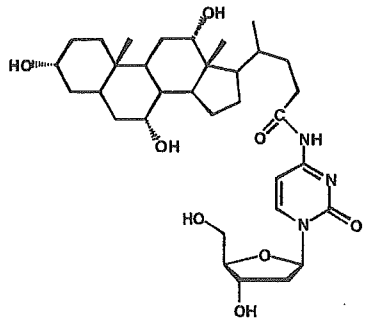

Figure 7. Chemical structure of N^4-cholyl-dC.

Mutagenic Activity of *N*-Nitroso Bile Acid Conjugates in *Salmonella* Strains. Mutagenic responses of *N*-nitroso bile acid conjugates in TA98 and TA100 were examined without metabolic activation. NO-TCA and NO-TDCA showed mutagenicity to TA100 in a dose-dependent manner but did not induce revertants in TA98. Their mutagenic activities were 9488 revertants for NO-TCA and 20800 revertants for NO-TDCA per μmol. Analysis of reverse mutations occurring at the *hisG46* site of TA100 with NO-TCA by DNA sequencing (Table 1) revealed G:C to A:T transitions dominantly. Among these, the pattern of CCC to CTC was almost four times higher than those of spontaneous mutations.

In Vivo Formation of Ethanesulfonic Acid-dC and N^4-Cholyl-dC. To confirm the formation of DNA adducts derived from bile acid conjugates in vivo, NO-TCA was singly injected at a dose of 250 mg/kg into Wistar rats by gavage, and then, 3-ethanesulfonic acid-dC and N^4-cholyl-dC were analyzed in the liver, glandular stomach, and colon mucosa, by a combination of HPLC separation and ^{32}P-postlabeling analysis. One hundred microgram aliquots of DNA digests were subjected to HPLC, and eluates were collected at 1 min intervals at retention times of 3−4 and 46−47 min, for the analysis of 3-ethanesulfonic acid-dC and N^4-cholyl-dC, respectively. The fractions were lyophilized and then analyzed by the ^{32}P-postlabeling method under nuclease P1 conditions. The adduct spot corresponding to the 3-ethanesulfonic acid-dC could be detected in the stomach and colon mucosa but not in the liver of rats treated with NO-TCA; no adduct spots were detected in these organs of control rats (Figure 9A). Adduct levels were estimated to be 0.22 ± 0.05 for stomach and 0.29 ± 0.09 for colon per 10^6 nucleotides. As the case of 3-ethanesulfonic acid-dC adduct, N^4-cholyl-dC adduct was seen in the stomach and colon mucosa of NO-TCA treated animals at estimated levels of 0.51 ± 0.33 and 0.67 ± 0.42 per 10^9 nucleotides, respectively (Figure 9B), although no adduct spot corresponding to N^4-cholyl-dC could be detected in fraction samples at a retention time of 46−47 min from control rats.

Discussion

The present study revealed formation and chemical structures of DNA adducts derived from *N*-nitroso bile acid conjugates using the ^{32}P-postlabeling method and various spectrometry techniques. Ethanesulfonic acid-dC adduct was formed from NO-TCA or NO-TDCA with calf thymus DNA or 2′-deoxynucleotides as a major adduct, and its chemical structure was concluded to be 3-ethanesulfonic acid-dC. In the case of reaction between NO-GCA with DNA, the major adducts were earlier demonstrated to be 7-carboxymethylguanine, 3-carboxymethyladenine,

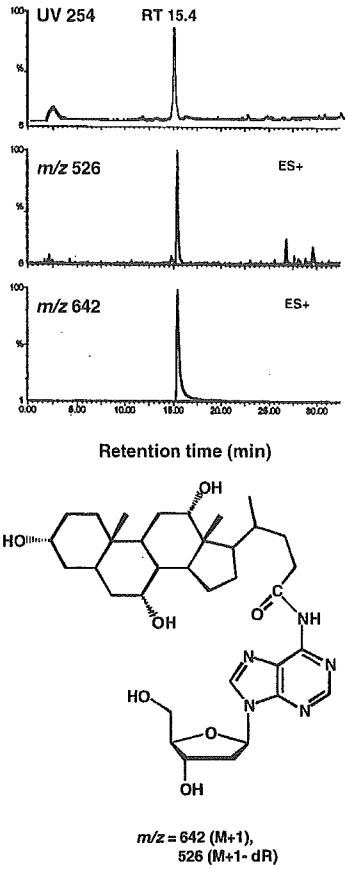

Figure 8. LC-ESI/MS analysis and chemical structure of the CA-dA adduct. An aliquot of purified CA-dA adduct was subjected on an analytical grade ODS column under the same conditions as used in CA-dC adduct and detected by UV (254 nm) absorption and ESI/MS (*m/z* 642 and 526, M + 1). Proposed mass of *m/z* = 642 corresponds to the $[M + H]^+$ of the N^6-cholyl-dA. A fragmentation at *m/z* 526 corresponded to the loss of the deoxyribose moiety from the original compound.

Table 1. Mutation Spectra for *hisG46* Reversions of TA100 Treated with NO-TCA

	TA100	
	control	NO-TCA
	G:C to A:T	
TCC (Ser)	11	11
CTC (Leu)	21	76
	G:C to T:A	
ACC (Thr)	37	13
CAC (His)	26	0
	G:C to C:G	
GCC (Ala)	5	0
%	100	100
no. of mutants	(19)	(53)

and O^6-carboxymethylguanine (*28*). As with formation of carboxymethyl-DNA adducts, ethanesulfonic acid adducts with other nucleotides than dC might be formed from NO-TCA and DNA. However, only a single spot could be detected in the reaction mixture of NO-TCA and 3′-dCp under the ^{32}P-postlabeling conditions used in the present study. On the other hand, several adducts containing a bile acid moieties were also formed from NO-TCA or NO-TDCA with calf thymus DNA or 2′-deoxyribonucleotides. The chemical structures of these major adducts were

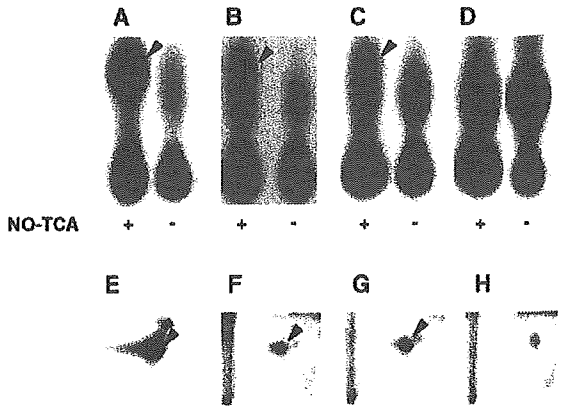

Figure 9. Autoradiograms of 3-ethanesulfonic acid-dC (A–D) and N^4-cholyl-dC (E–H) in calf thymus DNA or some organs of Wistar rats treated with or without NO-TCA. Adducts were analyzed by a combination of HPLC separation and ^{32}P-post-labeling analysis, as described in the Materials and Methods. Calf thymus DNA treated with NO-TCA (A, E) was used as a positive control. DNA samples were isolated from glandular stomach (B, F), colon mucosa (C, G), and liver (D, H) of rats with or without NO-TCA treatment. Adducts are indicated by the arrowheads.

concluded to be N^4-cholyl-dC, N^4-deoxycholyl-dC, and N^6-cholyl-dA, respectively, by spectrometry analysis. In addition, one minor adduct formed from NO-TCA and calf thymus DNA was suggested to be a dG adduct, although its chemical structure has yet to be clarified. Because the carbonyl moiety of CA was found to bind to N^4- or N^6-exocyclic amino groups of dC or dA in the present study, it is possible that the structure of CA-dG is N^2-cholyl-dG. In general, the positions of N7-, O6-dG, and N3-dA are preferentially attacked by alkylating agents, and 7-dG and 3-dA adducts are well-known to be unstable; thus, these adducts undergo spontaneous cleavage of the glycosidic bond, to produce abasic sites in DNA (*34*). Therefore, if 7-dG- or 3-dA-ethanesulfonic acid or bile acid adducts are produced from NO-TCA or NO-TDCA, they would be impossible to be detected by the ^{32}P-postlabeling methods used in the present study. As shown in Scheme 1, possible mechanisms for the formation of 3-ethanesulfonic acid-dC might be involved in the decomposition products of *N*-nitroso tauro bile acid conjugates. Dayal et al. have reported that *N*-nitroso bile acid conjugates decompose between pH 6 and pH 9 in aqueous buffered solutions, to generate several carcinogenic species, such as alkyl diazoate and its protonated form (*27*, *34*). Such electrophilic species might be implicated in the alkylation of DNA. In fact, the existence of electrophilic decomposition products of *N*-nitrosotauroursodeoxycholic acid, such as isethionic acid, diazoisethionic acid, and the protonated diazoate intermediate, has already been demonstrated by mass spectrum analysis (*27*). Meanwhile, there are no data regarding how bile acid-DNA adducts are formed at present; if the same mechanisms are involved in the generation of (deoxy)CA-DNA and ethanesulfonic acid-DNA, production of bile acid diazoate from NO-TCA or NO-TDCA would be necessary (Scheme 1). It has been well-known that the majority of the bulky-DNA adducts derived from exogenous mutagenic/carcinogenic compounds such as polycyclic aromatic hydrocarbons and heterocyclic amines have been identified as dG-C8 or dG-N2 adducts (*35*–*37*). However, in the present study, *N*-NO-bile acid conjugates preferentially

Scheme 1. Possible Reaction Mechanisms of *N*-Nitroso Bile Acid Conjugates and DNA

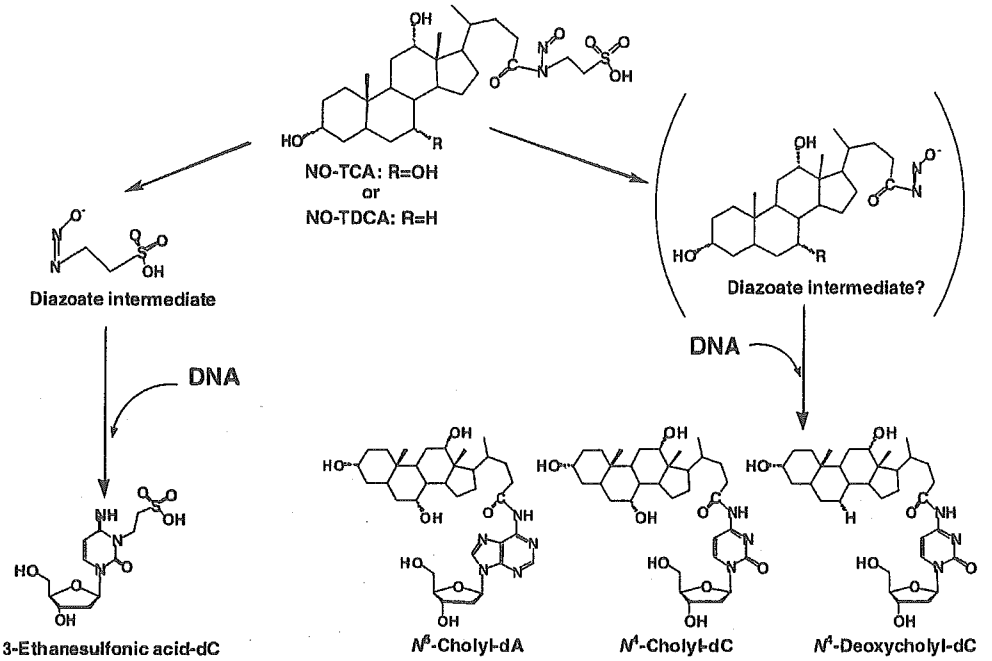

attacked the amino group at the N^4-position of dC and N^6-position of dA. Because the most reactive exocyclic amino group is known to be the N^4-position of dC, followed by the N^6-position of dA and the N^2-position of dG, it is likely that *N*-NO-bile acid conjugates could form N^4-cholyl-dC or N^6-cholyl-dA, rather than a dG adduct. Moreover, there are some reports describing the reaction between alkylating agents and cytidine or adenosine, and the N^3- and N^4-positions of dC and N^6-position of dA have been alkylated predominantly (*38*−*42*). In addition, the rearrangement of N^3-(deoxy)cholyl-dC or N^1-cholyl-dA to N^4-cholyl-dC or N^6-cholyl-dA is not ruled out. The mechanisms underlying formation of CA- or DCA-DNA adducts remain unclear. To understand the mechanisms for the formation of bile acid-DNA adducts, further study is needed.

Furthermore, we here demonstrated *N*-nitroso bile acid conjugates to induce mutations and their mutation spectrum in *S. typhimurium*. NO-TCA and NO-TDCA induced revertants to TA100, which detects base pair change mutations, but not in TA98, a detector of frameshift mutations. Moreover, NO-TCA induced G:C to A:T transitions predominantly in TA100, and most of them were CCC to CTC. This suggests that 3-ethanesulfonic acid- and N^4-cholyl-dC lead to G:C to A:T transitions. At present, there are no data to explain which adduct, ethanesulfonic acid- or CA-dC, is mainly responsible in TA100, and further studies are clearly warranted to clarify the mechanisms of mutagenicity.

When NO-TCA was injected to Wistar rats at a dose of 250 mg/kg, ethanesulfonic acid- and CA-DNA were detected in the glandular stomach and colon mucosa but not the liver, under the conditions used in the present study. While levels of these two kinds of adducts greatly differed, there was little variation between the two organ sites. Because the yield of CA-DNA in vitro was about 90 times lower than that of 3-ethanesulfonic acid-dC, it is reasonable that the yield of CA-DNA in vivo was also much lower than that of ethanesulfonic acid-DNA. Moreover, it has been reported that NO-TCA is not stable under physiological conditions and thus might easily produce the chemically active compound, alkyl diazoate, and inactive compounds, such as free bile acids (*27*). In the present study, NO-TCA was singly administered to rats by intragastric intubation and the stomach and colon mucosa would have been exposed to decomposition products. However, active compound apparently did not reach to the hepatic cells or only at very low levels. Alternatively, NO-TCA was efficiently inactivated by enzymes in the liver. It should be borne in mind that Busby et al. previously demonstrated NO-TCA to induce liver and stomach tumors in rats (*16*), with administration by gavage for 6 consecutive weeks with a total of 300 mg compound per rat. To clarify the tissue distribution of ethanesulfonic acid-dC and CA-DNA, an increase in the amount of NO-TCA and/or differing administration routes need to be explored.

Nitrosation of bile acid conjugates can be mediated by the acid-catalyzed reaction of amides with nitrite (*14*) and activated macrophages in infected and inflamed organs also believed to be involved in such reactions. Thus, nitrosated bile acid conjugates might contribute to human cancer development as endogenous mutagens. It is well-documented that G to A base substitutions are frequently observed in cancer related genes, such as *ras* family members and *p53* (*43*−*45*). Chemical instability might explain why nitroso bile acid derivatives have not been detected in any biological samples so far tested (*46*). Targeting specific DNA adducts, such as 3-ethanesulfonic acid-dC, N^4-cholyl-dC, N^4-deoxycholyl-dC, and N^6-cholyl-dA, therefore appears to be a useful way of monitoring endogenous formation of nitrosated bile acid conjugates. To clarify involvement of these nitroso bile acid conjugates in human carcinogenesis, it is clearly necessary to evaluate exposure levels.

Acknowledgment. This study was supported by Grants-in-Aid for Cancer Research from the Ministry of Health, Labor and Welfare of Japan and for scientific research from the Japan Society for the Promotion of Science. We acknowledge the contributions of Dr. T. Suzuki (Department of Biological Pharmacy School of Pharmacy, Shujitsu University) in useful discussions. S.E. is the recipient of a Research Resident fellowship from the Foundation of Promotion of Cancer Research.

Supporting Information Available: HMBC spectrum of ethanesulfonic acid-dC adduct and various spectral data of DCA-dC. This material is available free of charge via the Internet at http://pubs.acs.org.

References

(1) Debruyne, P. R., Bruyneel, E. A., Li, X., Zimber, A., Gespach, C., and Mareel, M. M. (2001) The role of bile acids in carcinogenesis. *Mutat. Res. 480–481*, 359–369.

(2) de Kok, T. M., and van Maanen, J. M. (2000) Evaluation of fecal mutagenicity and colorectal cancer risk. *Mutat. Res. 463*, 53–101.

(3) Owen, R. W. (1997) Faecal steroids and colorectal carcinogenesis. *Scand. J. Gastroenterol. 222* (Suppl.), 76–82.

(4) Kishida, T., Taguchi, F., Feng, L., Tatsuguchi, A., Sato, J., Fujimori, S., Tachikawa, H., Tamagawa, T., Yoshida, Y., and Kobayashi, M. (1997) Analysis of bile acids in colon residual liquid or fecal material in patients with cololectal neoplasia and control subjects. *J. Gastroenterol. 32*, 306–311.

(5) Deschner, E. E., Cohen, B. I., and Raicht, R. F. (1981) Acute and chronic effect of dietary cholic acids on colonic epithelial cell proliferation. *Digestion 21*, 290–296.

(6) Bartram, H. P., Scheppach, W., Schmid, H., Hofmann, A., Dusel, G., Richter, F., Richter, A., and Kasper, H. (1993) Proliferation of human colonic mucosa as an intermediate biomarker of carcinogenesis: Effects of butyrate, deoxycholate, calcium, ammonia, and pH. *Cancer Res. 53*, 3283–3288.

(7) Mcmillan, L., Butcher, S., Wallis, Y., Neoptolemos, J. P., and Lord, J. M. (2000) Bile acids reduce the apoptosis-inducing effects of sodium butyrate on human colon adenoma (AA/CC) cells: Implication for colon carcinogenesis. *Biochem. Biophys. Res. Commun. 273*, 45–49.

(8) Narisawa, T., Magadia, N. E., Weisburger, J. H., and Wynder, E. L. (1974) Promoting effect of bile acids on colon carcinogenesis after intrarectal instillation of *N*-methyl-*N'*-nitrosoguanidine in rats. *J. Natl. Cancer Inst. 53*, 1093–1097.

(9) Reddy, B. S., Watanabe, K., Weisburger, J. H., and Wynder, E. L. (1977) Promoting effect of bile acids in colon carcinogenesis in germ-free and conventional F344 rats. *Cancer Res. 37*, 3228–3242.

(10) Hamada, K., Umemoto, A., Kajikawa, A., Seraj, M. J., and Monden, Y. (1994) *In vitro* formation of DNA adducts with bile acids. *Carcinogenesis 15*, 1911–1915.

(11) Scates, D. K., Spigelman, A. D., and Venitt, S. (1994) Bile acids do not form adducts when incubated with DNA in vitro. *Carcinogenesis 15*, 2945–2948.

(12) Scates, D. K., Spigelman, A. D., and Venitt, S. (1995) Appearance of artifacts when using ^{32}P-postlabeling to investigate DNA adduct formation by bile acids in vitro: Lack of evidence for covalent binding. *Carcinogenesis 16*, 1489–1491.

(13) Scates, D. K., Spigelman, A. D., Phillips, R. K. S., and Venitt, S. (1997) The use of ^{32}P-postlabeling in studies of the nature and origin of DNA adducts formed by bile from patients with familial adenomatous polyposis and from normal patients. *Mutat. Res. 378*, 113–125.

(14) Shuker, D. E. G., Tannenbaum, S. R., and Wishnok, J. S. (1981) *N*-Nitroso bile acid conjugates. 1. Synthesis, chemical reactivity, and mutagenic activity. *J. Org. Chem., 46*, 2092–2096.

(15) Puju, S., Shuker, D. E. G., Bishop, W. W., Falchuk, K. R., Tannenbaum, S. R., and Thilly, W. G. (1982). Mutagenicity of *N*-nitroso bile acid conjugates in *Salmonella typhimurium* and diploid human lymphoblasts. *Cancer Res. 42*, 2601–2604.

(16) Busby, W. F., Shuker, D. E. G., Charley, G., Newberne, P. M., Tannenbaum, S. R., and Wogan, G. N. (1985) Carcinogenicity in rats of the nitrosated bile acid conjugates: *N*-Nitrosoglycocholic acid and *N*-nitrosotaurocholic acid. *Cancer Res. 45*, 1367–1371.

(17) Miwa, K., Hasegawa, H., Fujimura, T., Matsumoto, H., Miyata, R., Kosaka, T., Miyazaki, I., and Hattori, T. (1992) Duodenal reflux through the pylorus induces gastric adenocarcinoma in the rat. *Carcinogenesis 13*, 2313–2316.

(18) Miwa, K., Kinami, S., Miyazaki, I., and Hattori, T. (1996) Positive association between dietary fat intake and risk of gastric stump carcinoma in rats. *Carcinogenesis 17*, 1885–1889.

(19) Kumagai, H., Mukaisyo, K., Sugihara, H., Miwa, K., Yamamoto, G., and Hattori, T. (2004) Thioproline inhibits development of esophageal adenocarcinoma induced by gastroduodenal reflux in rats. *Carcinogenesis 25*, 723–727.

(20) Caygill, C. P., Hill, M. J., Kirkham, J. S., and Northfield, T. C. (1986) Mortality from gastric cancer following gastric surgery for peptic ulcer. *Lancet 1*, 929–931.

(21) Viste, A., Bjornestad, E., Opheim, P., Skarstein, A., Thunold, J., Hartveit, F., Eide, G. E., Eide, T. J., and Soreide, O. (1986) Risk of carcinoma following gastric operations for benign disease: A historical cohort study of 3470 patients. *Lancet 2*, 502–504.

(22) Lundegardh, G., Adami, H. O., Helmick, C., Zack, M., and Meirik, O. (1988) Stomach cancer after partial gastrectomy for benign ulcer disease. *N. Engl. J. Med. 319*, 195–200.

(23) Toftgaard, C. (1989) Gastric cancer after peptic ulcer surgery. A historic prospective cohort investigation. *Ann. Surg. 210*, 159–164.

(24) Street J. M., Trafford, D. J. H., and Makin H. L. J. (1983) The quantitative estimation of bile acids and their conjugates in human biological fluids. *J. Lipid Res. 24*, 491–511.

(25) Scalia, S. (1988) Simultaneous determination of free and conjugated bile acids in human gastric juice by high-performance liquid chromatography. *J. Chromatogr. 431*, 259–269.

(26) Mirvish, S. S. (1995) Role of *N*-nitroso compounds (NOC) and *N*-nitrosation in etiology of gastric, esophageal, nasopharyngeal and bladder cancer and contribution to cancer of known exposures to NOC. *Cancer Lett. 93*, 17–48.

(27) Dayal, B., and Ertel, N. H. (1997) Studies on *N*-nitroso bile acid amides in relation to their possible role in gastrointestinal cancer. *Lipids 32*, 1331–1340.

(28) Shuker, D. E. G., and Margison, G. P. (1997) Nitrosated glycine derivatives as a potential source of O^6-methylguanine in DNA. *Cancer Res. 57*, 366–369.

(29) Takamura, T., Sugimura, T., and Wakabayashi, K. (2004) Formation of DNA adducts by reactive intermediates, bile acid-adenylate. Proceedings of 63rd Annual Meeting of the Japanese Cancer Association, p 85.

(30) Reddy, M. V., and Randerath, K. (1986) Nuclease P1-mediated enhancement of sensitivity of ^{32}P-postlabeling test for structurally diverse DNA adducts. *Carcinogenesis 7*, 1543–1551.

(31) Takamura-Enya, T., Watanabe, M., Totsuka, Y., Kanazawa, T., Matsushima-Hibiya, Y., Koyama, K., Sugimura, T., and Wakabayashi, K. (2001) Mono(ADP-ribosyl)ation of 2′-deoxyguanosine residue in DNA by an apoptosis-inducing protein, pierisin-1, from cabbage butterfly. *Proc. Natl. Acad. Sci. U.S.A. 98*, 12414–12419.

(32) Gupta, R. C. (1985) Enhanced sensitivity of ^{32}P-post-labeling analysis of aromatic carcinogen: DNA adducts. *Cancer Res. 45*, 5656–5662.

(33) Yahagi, T., Nagao, M., Seino, Y., Matsushima, T., Sugimuta, T., and Okada, M. (1977) Mutagenicities of *N*-nitrosoamines on *Salmonella*. *Mutat. Res. 48*, 121–130.

(34) Dayal, B., Bhojawala, J., Rapole, K. R., Pramanik, B. N., Ertel, N. H., Shefer, S., and Salen, G. (1996) Chemical synthesis, structural analysis, and decomposition of *N*-nitroso bile acid conjugates. *Bioorg. Med. Chem. 4*, 885–890.

(35) Chen, S. C., Hilton, B. D., Roman, J. M., and Dipple, A. (1989) DNA adducts from carcinogenic and noncarcinogenic enantiomers of benzo[*a*]pyrene dihydrodiol epoxide. *Chem. Res. Toxicol.* 2, 334–340.

(36) Sayer, J. M., Chadha, A., Agarwal, H. S. K., Yeh, H. J. C., Yagi, H., and Jerina, D. M. (1991) Covalent nucleoside adducts of benzo-[*a*]pyrene 7,8-diol 9,10-epoxides: Structural reinvestigation and characterization of a novel adenosine adduct on the ribose moiety. *J. Org. Chem. 56*, 20–29.

(37) Snyderwine, E. G., and Turteltaub, K. W. (2000) Interactions with cellular macromolecules. In *Food Borne Carcinogenic Heterocyclic Amines* (Nagao, M., and Sugimura, T., Eds.) pp 131–161, John Wiley & Sons Ltd., West Sussex.

(38) Brookes, P., and Lawley, P. D. (1962) The methylation of cytosine and cytidine. *J. Chem. Soc.* 1348.

(39) Sun, L., and Singer, B. (1974) Reaction of cytidine with ethylating agents. *Biochemistry 13*, 1905–1913.

(40) Singer, B., Sun, L., and Fraenkel-Conrat, H. (1974) Reaction of adenosine with ethylating agents. *Biochemistry 13*, 1913–1920.

(41) Singer, B. (1976) O^2-Alkylcytidine—A new major product of neutral, aqueous reaction of cytidine with carcinogens. *FEBS Lett. 63*, 85–88.
(42) Segal, A., Solomon, J. J., Mignano, J., and Dino, J. (1981) The isolation and characterization of 3-(2-carboxyethyl)cytosine following in vitro reaction of b-propiolactone with calf thymus DNA. *Chem. Biol. Interact. 35*, 349–361.
(43) Smith, G., Crey, F. A., Beattie, J., Wilkie, M. J., Lightfoot, T. J., Coxhead, J., Garner, R. C., Steele, R. J. C., and Wolf, R. (2002) Mutations in APC, Kirsten-ras, and p53-alternative genetic pathways to colorectal cancer. *Proc. Natl. Acad. Sci. U.S.A. 99*, 9433–9438.
(44) Gealy, R., Zhang, L., Siegfried, J. M., Luketich, J. D., and Keohavong, P. (1999) Comparison of mutations in the p53 and K-ras genes in lung carcinomas from smoking and nonsmoking women. *Cancer Epidemiol., Biomarkers Prev. 8*, 297–302.
(45) Olivier, M., Hussain, S. P., de Fromentel, C. C., Hainaut, P., and Harris, C. C. (2004) TP53 mutation spectra and load: A tool for generating hypotheses on the etiology of cancer. In *Mechanisms of Carcinogenesis: Contributions of Molecular Epidemiology* (Buffler, P., Rice, J., Baan, R., Bird, M., and Boffetta, P., Eds.) IARC Scientific Publications No. 157, pp 247–270, IARC, Lyon.
(46) Fein, M., Fuchs, K.-H., Stopper, H., Diem, S., and Herderich, M. (2000) Duodenogastric reflux and foregut carcinogenesis: Analysis of duodenal juice in a rodent model of cancer. *Carcinogenesis 21*, 2079–2083.

TX050144X

Formation of DNA Adducts with Cholyl Adenylate, a Putative Intermediate for Biosynthesis of Cholyl-CoA

Takeji Takamura-Enya, Nariyasu Mano, Nobuo Kawahara, Junichi Goto, and Keiji Wakabayashi

Cancer Prevention Basic Research Project, National Cancer Center Research Institute, 5-1-1 Tsukiji, Chuo-ku, Tokyo 104-0045, Japan, Graduate School of Pharmaceutical Sciences, Tohoku University, Aobayama, Aoba-ku, Sendai 980-8578, Japan, Department of Pharmaceutical Sciences, Tohoku University Hospital, 1-1 Seiryo-machi, Aoba-ku, Sendai 980-8574, Japan, and National Institute of Health Sciences, 18-1, Kamiyoga 1-chome, Setagaya-ku, Tokyo 158-8501, Japan

Chemical Research in Toxicology®

Reprinted from
Volume 18, Number 11, Pages 1715–1720

P-166

Formation of DNA Adducts with Cholyl Adenylate, a Putative Intermediate for Biosynthesis of Cholyl-CoA

Takeji Takamura-Enya,*,† Nariyasu Mano,‡ Nobuo Kawahara,§ Junichi Goto,‡,|| and Keiji Wakabayashi†

Cancer Prevention Basic Research Project, National Cancer Center Research Institute, 5-1-1 Tsukiji, Chuo-ku, Tokyo 104-0045, Japan, Graduate School of Pharmaceutical Sciences, Tohoku University, Aobayama, Aoba-ku, Sendai 980-8578, Japan, Department of Pharmaceutical Sciences, Tohoku University Hospital, 1-1 Seiryo-machi, Aoba-ku, Sendai 980-8574, Japan, and National Institute of Health Sciences, 18-1, Kamiyoga 1-chome, Setagaya-ku, Tokyo 158-8501, Japan

Received June 15, 2005

Cholyl adenylate is a putative intermediate for biosynthesis of cholic acid-coenzyme A (CoA) thioester conjugates by acyl-CoA synthetase. Early studies showed the conjugated acid anhydride moiety of cholyl adenylate to be reactive, attacking proteins to form protein-cholic acid adducts. In the present study, to clarify reactions of cholyl adenylate with DNA under physiological conditions, products with nucleosides were analyzed. HPLC-MS analyses indicated cholyl adenylate to primarily attack hydroxy groups of ribose moieties of nucleosides. Moreover, as speculated from UV and MS studies, exocyclic amino groups of 2′-deoxycytidine and 2′-deoxyadenosine were found to serve as targets of cholyl adenylate; the corresponding cholic amides, N^4-cholyl-2′-deoxycytidine and N^6-cholyl-2′-deoxyadenosine, were formed at yields of 0.32 and 0.06%, respectively. Structures of these base modified adducts were confirmed by direct comparison with synthetic compounds obtained from coupling reactions of cholic acid with each nucleoside in the presence of dicyclohexylcarbodiimide in pyridine at 70 °C. N^4-Cholyl-2′-deoxycytidine was also obtained at a level of 1.6 adducts per 10^5 nucleosides from enzymatic hydrolysates of calf thymus DNA reacted with cholyl adenylate. These results suggest that cholyl adenylate, released from CoA synthetase, may have some possibility as a DNA modifier in vivo.

Introduction

Bile acids are synthesized de novo in the liver from cholesterol and conjugated with glycine or taurine. They are stored in the gall bladder and excreted into the upper intestinal tract to promote absorption of dietary lipid materials by micellar formation. Most are reabsorbed from the ileum-proximal colon and returned to the liver. Remaining bile acids are changed by intestinal bacteria to secondary bile acids, which are absorbed in the colon to join in the enterohepatic circulation (*1*, *2*).

It has been postulated that bile acids play some role in carcinogenesis, especially contributing to the risk of colon cancer (*3*, *4*). Unconjugated deoxycholic acid and chenodeoxycholic acid have promoting effects on colon cancer development in rodent carcinogenesis models (*5*, *6*), and concentrations of bile acids have been reported to be elevated in patients with adenomatous polyps or colon cancer (*7*, *8*). Bile from familial adenomatous polyposis patients was further shown to contain constituents that form DNA adducts (*9*). In vitro direct modification of DNA with some bile acids was also demonstrated with ^{32}P-postlabeling methods (*10*). Moreover, mutagenicity of polycyclic aromatic hydrocarbons is reported to be enhanced with glycocholic acid and taurodeoxycholic acid (*11*), and comet assays have revealed DNA damage in cells treated with deoxycholic acid (*12*). However, there have been no reports of determination of chemical structures of DNA adducts modified with bile acids.

Cholyl adenylate is a putative intermediate in the biosynthesis of CoA thioester conjugates of cholic acid, one of the primary bile acids synthesized in the liver and excreted as a taurine or glycine conjugate (*13*−*16*) (Scheme 1). During synthesis of the amino acid conjugates, cholic acid is converted to a corresponding coenzyme A (CoA)[1] thioester by the catalytic action of acyl-CoA synthetase, followed by amide formation with amino acids catalyzed by *N*-acyltransferase (*1*, *2*, *17*−*19*). Generally, CoA thioester formation in acyl-CoA synthetases affords an acyl adenylate as a highly active intermediate where the adenosine monophosphate (AMP) moiety of ATP is covalently transferred to a carboxyl group of substrates (*20*, *21*). Cholyl adenylate is, thus, a putative intermediate during the synthesis of CoA thioesters. Formation of this intermediate is well-documented from in vitro experiments where cholic acid was converted to cholyl adenylate by cell extracts of intestinal *Eubacterium* and also by a rat liver microsomal fraction (*13*). It has also been shown that cholyl adenylate is sufficiently

* To whom correspondence should be addressed. Tel: +81-3-3547-5201 ext. 4354. Fax: +81-3-3543-9305. E-mail: tenya@gan2.res.ncc.go.jp.
† National Cancer Center Research Institute.
‡ Tohoku University.
§ National Institute of Health Sciences.
|| Tohoku University Hospital.

[1] Abbreviations: CoA, coenzyme A; dA, 2′-deoxyadenosine; dC, 2′-deoxycytidine; dG, 2′-deoxyguanosine; T, thymidine; DCC, dicyclohexylcarbodiimide; THF, tetrahydrofuran; TBAF, tetrabutylammonium fluoride.

10.1021/tx050159v CCC: $30.25
Published on Web 09/29/2005

Scheme 1. In Vivo Pathway of Formation of Amino Acid Conjugates of Cholic Acid

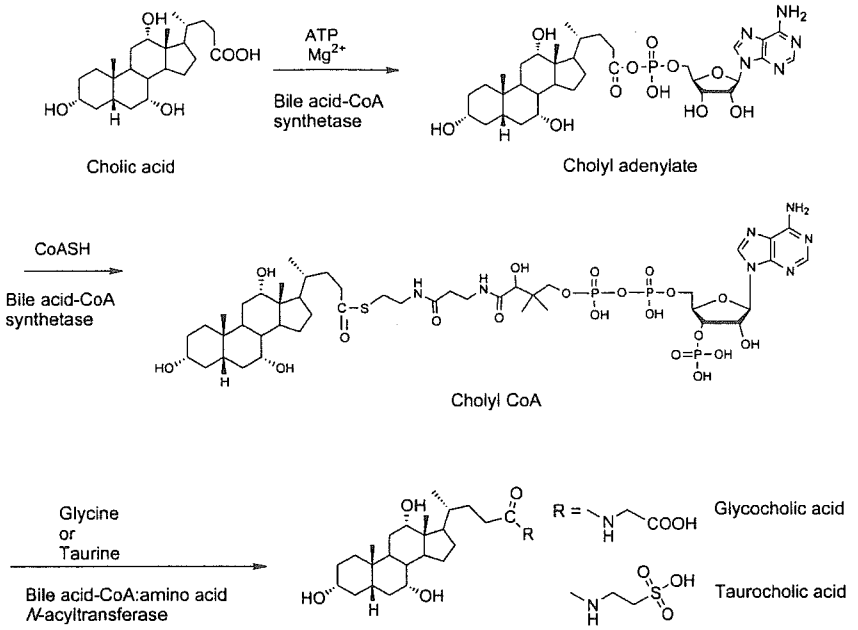

reactive to attack taurine nonenzymatically (*13*). Moreover, reactions of cholyl adenylate with lysozyme clearly yield protein-bound cholic acids involving lysine residues at codons 1, 33, 97, and 116 (*15*). As an analogous bile acid-adenylate compound, deoxycholyl adenylate has also been demonstrated to form protein adducts with histone H3 (*16*). Bile acid-protein adducts were already found in in vivo samples, implicating the probable presence of a corresponding bile acid-adenylate intermediate in vivo (*22*).

Considering its reactivity and acid anhydride nature, cholyl adenylate would be expected to attack cellular DNA to form DNA adducts. In the present study, we analyzed reaction products of nucleosides and found cholyl adenylate to attack exocyclic amino groups of 2′-deoxycytidine (dC) and 2′-deoxyadenosine (dA). The structures of the resulting nucleoside adducts were further confirmed by direct comparison of independent synthetic adducts. In addition, dC-cholic acid adducts were found to be formed by reactions of calf thymus DNA with cholyl adenylate. On the basis of these results, possible in vivo formation of DNA adducts with cholic acid is discussed.

Experimental Procedures

Materials. Cholyl adenylate was synthesized as described earlier (*13*), and its purity was determined to be 98% by LC-MS analysis. The main impurities were cholic acid and AMP, formed by decomposition. Calf thymus DNA, dC, dA, 2′-deoxyguanosine (dG), thymidine (T), and bovine intestinal and bacterial alkaline phosphatases were all from Sigma Chemical Co. (St. Louis, MO). ^{1}H NMR, ^{13}C NMR, ^{1}H−^{1}H-correlated spectroscopy (2D-COSY), heteronuclear multiple quantum coherence (HMQC), and heteronuclear multiple bond correlations (HMBCs) were recorded on a JEOL α-600 (600 MHz) or a JEOL α-500 (500 MHz) spectrometer. Chemical shifts are reported in parts per million (ppm), and J values are given in Hz. HPLC-ESI-MS was performed with a Waters ZQ 2000 mass single stage spectrometer equipped with an Agilent 1100 HPLC system.

Reaction of Deoxynucleosides and Cholyl Adenylate. Aliquots of dC, dG, dA, or T (40 mM) were incubated with cholyl adenylate (20 mM) at 37 °C, pH 7.0, in 100 mM phosphate buffer. The overnight reaction mixture was then applied to LC-ESI-MS on an ODS column (Imtakt Cadenza CD-C18, 4.6 mm × 75 mm, Kyoto, Japan) with a linear gradient during the course of 30 min from 0 to 80% acetonitrile in 50 mM HCOOH−NH_4-OH buffer solution at pH 7.0 with a flow rate of 1.0 mL/mim. ESI-MS analysis of total current chromatographs was performed with positive ion detection with a cone voltage of 30 V. Selective molecular ions of *m/z* 618 for dC modified with cholic acid, *m/z* 641 for dA modified with cholic acid, *m/z* 658 for dG modified with cholic acid, and *m/z* 632 for T modified with cholic acid were monitored at a cone voltage of 30 V with positive ion detection. Molecular ions arising from loss of the deoxyribose moiety from the parent compounds (*m/z* 116 minus from mass of the parent compounds) were monitored with sequential rapid exchange of the initial cone voltage of 30−50 V. UV chromatograms were also recorded at a wavelength of 260 nm.

Reaction of Calf Thymus DNA with Cholyl Adenylate. Calf thymus DNA (2 mg) was reacted with cholyl adenylate (20 mM) at 37 °C in 1 mL of 100 mM phosphate buffer (pH 7.0) for 24 h. After the reaction, DNA was recovered by ethanol precipitation and digested enzymatically to nucleosides with deoxyribonuclease I, followed by alkaline phosphatase and phosphodiesterase I (*23*). The reaction mixture was then extracted with water-saturated butanol, and the organic layer was recovered and evaporated. Residues were redissolved in 20% acetonitrile and subjected to HPLC conditioned as for the analysis of nucleosides with cholyl adenylate.

Synthesis of N^4-Cholyl-2′-deoxycytidine. A mixture of 0.1 mmol of 3′,5′-bis-*O*-*tert*-butyldimethylsilyl-2′-deoxycitiydine, obtained with a published method (*24*), cholic acid (0.1 mmol), and dicyclohexylcarbodiimide (DCC, 0.12 mmol) in pyridine (10 mL) was stirred at 70 °C for 4 h. After the precipitate was filtered off, the solvent was evaporated. The residue was applied to silica gel column chromatography (35 mm × 250 mm) with a stepwise gradient of methanol/chloroform (0−20%) to give silyl-protected N^4-cholyl-dC as a white solid. This material was dissolved in 5 mL of tetrahydrofuran (THF) and further treated with 1 M tetrabutylammonium fluoride (TBAF) in THF (500 μL). After the reaction mixture was stirred overnight at room temperature and then evaporated, the residue was further purified by column chromatography using ODS (26 mm × 300 mm) with methanol/water (10−80%) to give the desired compound as a white solid with a yield of 20%. ^{1}H NMR (500 MHz, DMSO-d_6): δ 10.79 (s, 1H, NHCO), 8.29 [d, J = 7.5 Hz, 1H, H-6 (dC)], 7.19 [d, J = 7.5 Hz, 1H,H-5 (dC)], 6.09 [t, J = 6.2 Hz, 1H, H-1′(dR)], 5.24 [brs, 1H, 3′-OH (dR)], 5.06 [brs, 1H, 5′-OH (dR)], 4.27 [d, J = 4.5 Hz,

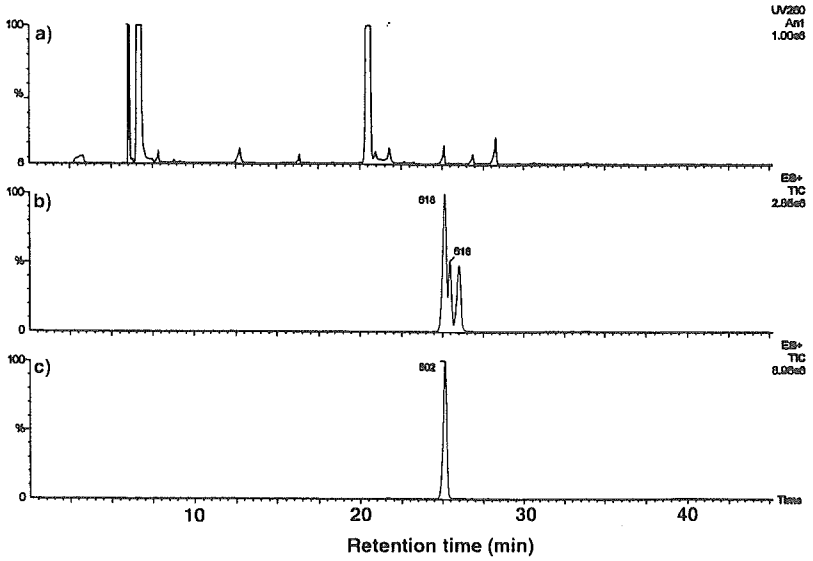

Figure 1. LC-ESI-MS chromatogram of reaction products of cholyl adenylate with dC. Cholyl adenylate (20 mM) was incubated with dC (20 mM) at 37 °C, pH 7.0, in 100 mM phosphate buffer. The overnight reaction mixture was then applied to LC-ESI-MS. HPLC conditions are shown in the Experimental Procedures. (a) UV chromatogram at 260 nm; (b) selected ion monitoring at *m/z* 618, which is estimated to be a molecular ion of dC modified with cholic acid; and (c) selected ion monitoring at *m/z* 502 derived from loss of the deoxyribose moiety from the parent dC-cholic acid adduct with a molecular ion of *m/z* 618.

1H, 3-OH(CA)], 4.20 [dt, J = 3.5, 5.5 Hz, 1H, H-3′(dR)], 4.07 [d, J = 3.0 Hz, 1H, 12-OH (CA)], 3.97 [d, J = 3.0 Hz, 1H, 7-OH (CA)], 3.84 [dt, J = 3.5, 4.0 Hz, 1H, H-4′(dR)], 3.77 [brs, 1H, H-12(CA)], 3.65−3.53 [m, 3H, H-7(CA), H-5′, 5″(dR)], 3.25−3.13 [m, 1H, H-3(CA)], 2.45−2.14 [m, 5H, H-4α, −9, −23α, −23β-(CA), H-2′(dR)], 2.03−1.94 [m, 2H, H-14(CA), H-2″(dR)], 1.86−1.52 (m, 7H, H-17, 20, 22α, 16α, H-1α, H-6β, H-15β), 1.48−1.25 (m, 12H, H-2α, −2β, 4β, 5, 6α, 8, 11α, 11β, 15α, 16β, 22β), 1.0−0.92 (m, 1H, H-1β), 0.91 [d, J = 6.0 Hz, 3H, CH_3-21(CA)], 0.79 [s, 3H, CH_3-19(CA)], 0.57 [s, 3H, CH_3-18(CA)]. ^{13}C NMR (125 MHz, DMSO-d_6): δ 174.4 [C=O(CA)], 162.3 [C-2(dC, C=O)], 154.4 [C-4(dC)], 144.8 [C-6(dC)], 95.2 [C-5(dC)], 87.6 [C-4′(dR)], 86.1 [C-1′(dR)], 70.9 [C-12(CA)], 70.4 [C-3(CA)], 69.9 [C-3′(dR)], 66.2 [C-7(CA)], 60.9 [C-5′(dR)], 46.2 [C-17(CA)], 45.7 [C-13(CA)], 41.5 [C-5(CA)], 41.3 [C-14(CA)], 40.8 [C-2′(dR)], 40−39 [C-4, −8 (CA) overlapped with the absorbance signal of DMSO], 35.3 [C-1(CA)], 35.1 [C-20(CA)], 34.8 [C-6(CA)], 34.3 [C-10(CA)], 33.7 [C-23(CA)], 30.9 [C-22(CA)], 30.4 [C-2(CA)], 28.5 [C-11(CA)], 27.2 [C-16(CA)], 26.2 [C-9(CA)], 22.7 [C-15(CA)], 22.6 [C-19(CA)], 13.4 [C-21(CA)], 12.3 [C-18(CA)]. ESI-MS *m/z* 618, 502. UV λ_{max} 243, 295 nm.

Synthesis of N^6-Cholyl-2′-deoxyadenosine. The same procedures described for N^4-cholyl-2′-deoxycytidine were performed with 3′,5′-bis-*O*-*tert*-butyldimethylsilyl-2′-deoxyadenosine (*25*) instead using 3′,5′-bis-*O*-*tert*-butyldimethylsilyl-2′-deoxycytidine. The desired compound was obtained at a yield of 7%. ^{1}H NMR (600 MHz, DMSO-d_6): δ 10.58 (s, 1H, NHCO), 8.62 [s, H-8(dA)], 8.61 [s, H-2(dA)], 6.43 [t, J = 6.6 Hz, 1H, H-1′-(dR)], 5.32 [brs, 1H, 3′-OH (dR)], 4.98 [brs, 1H, 5′-OH (dR)], 4.42 [brs, 1H, H-3′(dR)], 4.27 [d, J = 4.8 Hz, 1H, 3-OH(CA)], 4.07 [d, J = 3.6 Hz, 1H, 12-OH (CA)], 3.97 [d, J = 3.6 Hz, 1H, 7-OH (CA)], 3.88 [dt, J = 3.0, 4.2 Hz, 1H, H-4′(dR)], 3.79 [brs, 1H, H-12(CA)], 3.55−3.41 [m, 3H, H-7(CA), H-5′, 5″(dR)], 3.25−3.13 [m, 1H, H-3(CA)], 2.75 [dt, J = 6.0, 13.2, 1H, H-2′(dR)], 2.59 [ddd, J = 4.8, 9.6, 14.4 Hz, 1H, H-23α(CA)], 2.48−2.45 [m, 1H, H-23β(CA)], 2.32 [ddd, J = 4.8, 6.0, 13.2 Hz, 1H, H-2″(dR)], 2.21 (dt, J = 12.0, 14.2 Hz, 1H, H-4α), 2.14 [dt, J = 4.8, 12.0 Hz, 1H, H-9(CA)], 1.99 (ddd, J = 7.2, 12.1, 12.1 Hz, 1H, H-14), 1.86−1.52 (m, 7H, H-17, 20, 22α, 16α, H-1α, H-6β, H-15β), 1.48−1.25 (m, 12H, H-2α, −2β, 4β, 5, 6α, 8, 11α, 11β, 15α, 16β, 22β), 0.96 [d, J = 7.2 Hz, 3H, CH_3-21(CA)], 0.96−0.92 (m, 1H, H-1β), 0.80 [s, 3H, CH_3-19(CA)], 0.59 [s, 3H, CH_3-18(CA)]. ^{13}C NMR (150 MHz, DMSO-d_6): δ 172.0 [C=O(CA)], 162.3 [C-2(dC, C=O)], 151.5 [(C-2(dA)], 151.4 [C-4(dA)], 149.6 [C-6(dA)], 142.5 [C-8(dA)], 123.8 [C-5(dA)], 87.9 [C-4′(dR)], 83.7 [C-1′(dR)], 71.0 [C-12(CA)], 70.6 [C-3(CA)], 70.4 [C-3′(dR)], 66.2 [C-7(CA)], 61.6 [C-5′(dR)], 46.2 [C-17(CA)], 45.7 [C-13(CA)], 41.5 [C-5(CA)], 41.3 [C-14(CA)], 40−39 [C-4, −8(CA), C-2′(dR) overlapped with the absorbance signal of DMSO], 35.3 [C-1(CA)], 35.1 [C-20(CA)], 34.8 [C-6(CA)], 34.3 [C-10(CA)], 33.4 [C-23(CA)], 31.0 [C-22(CA)], 30.4 [C-2(CA)], 28.5 [C-11(CA)], 27.2 [C-16(CA)], 26.2 [C-9(CA)], 22.7 [C-15(CA)], 22.6 [C-19(CA)], 17.1 [C-21(CA)], 12.3 [C-18(CA)]. ESI-MS *m/z* 642, 526. UV λ_{max} 272 nm.

Results and Discussion

When cholyl adenylate was incubated with dG, dA, dC, and T at 37 °C for 24 h, in each reaction mixture, two (for dG and T) or three new peaks (for dC and dA) were observed in HPLC chromatograms detected at a wavelength of 260 nm after a retention time of 15 min; these peaks were not observed in control reaction mixtures without nucleosides. Each of these peaks had a molecular ion corresponding to dehydrated condensation products between the cholic acid and the nucleobase (*m/z* = cholic acid + nucleobase − H_2O). Judging from integrated knowledge of the reactivity of nucleobases with acid anhydride, the reaction sites of nucleobases toward cholyl adenylate are probably the hydroxy groups of ribose moieties and amino groups of the base moieties, generating esters or amides of cholic acid, respectively. Among the peaks that appeared in the HPLC chromatograms of the reaction mixture, our current interest is modification of the base rather than the deoxyribose moiety, because hydroxy groups in the latter are generally fully protected with phosphorous acid in DNA molecules. With the aid of LC-ESI-MS analyses, we were able to select base modification peaks, which always accompanied the molecular ion peaks derived from the elimination of the deoxyribose moiety from the parent compounds. With reaction mixtures of dG or T with cholyl adenylate, the desired peaks were not obtained, indicating that only the deoxyribose moiety was modified with cholyl adenylate. On the other hand, in the reaction mixtures with dC or dA, base modification peaks were clearly observed. The yield of formation of the base-modified dC adduct was about 0.32%, which was about five times higher than that

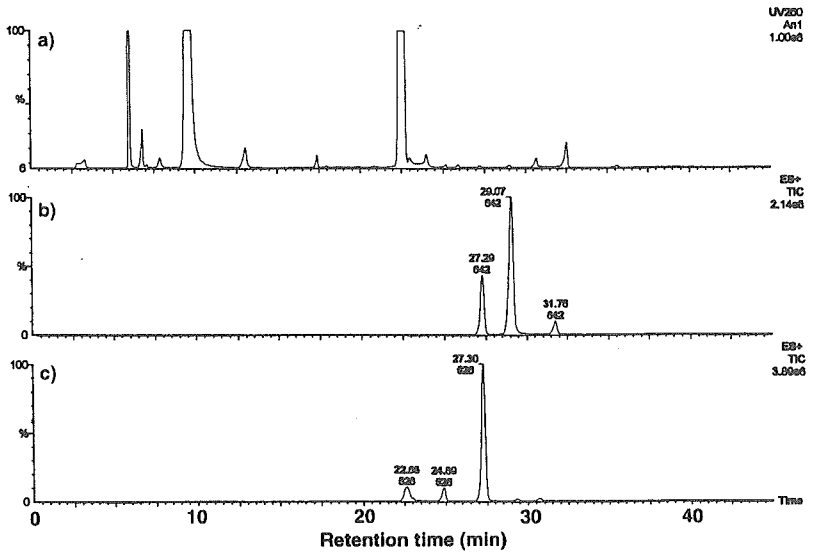

Figure 2. LC-ESI-MS chromatogram of reaction of cholyl adenylate with dA. Cholyl adenylate (20 mM) was incubated with dA (20 mM) at 37 °C, pH 7.0, in 100 mM phosphate buffer. The overnight reaction mixture was then applied to LC-ESI-MS. HPLC conditions are shown in the Experimental Procedures. (a) UV chromatogram at 260 nm; (b) selected ion monitoring at *m/z* 642, which is estimated to be a molecular ion of dA modified with cholic acid; and (c) selected ion monitoring at *m/z* 526, derived from loss of the deoxyribose moiety from the parent dA-cholic acid adduct with a molecular ion of *m/z* 642.

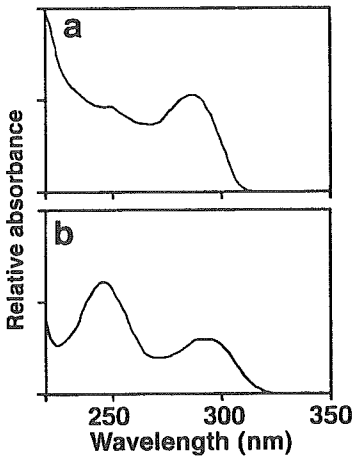

Figure 3. UV spectra of dC (a) and of an adduct from dC with cholyl adenylate (b) recorded on a Shimadzu VPD photoodiode array detector.

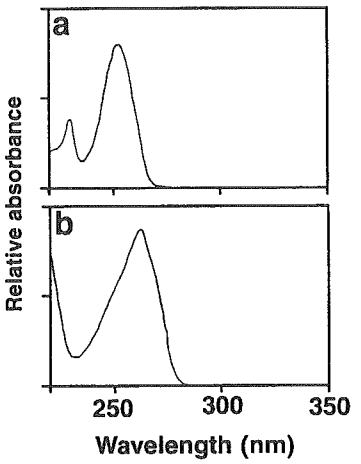

Figure 4. UV spectra of dA (a) and of an adduct from dA with cholyl adenylate (b) recorded on a Shimadzu VPD photoodiode array detector.

of the dA adduct (0.06%), as estimated from chromatograms of UV absorbance at 260 nm. The reaction of dC with cholyl adenylate yielded a base modified compound at a retention time of 25.0 min on HPLC chromatograms, with a molecular ion peak of *m/z* 618 accompanied with 502 (*m/z* 618-dR) (Figure 1). In the case of dA with cholyl adenylate, a peak was detected at a retention time in 27.3 min with molecular ion peaks of *m/z* 642 and 526 (*m/z* 642-dR) (Figure 2). The UV spectra of these adducts were drastically changed from those of the original compounds and were similar to the patterns of acyl amides of dC and dA, indicating cholyl adenylate to attack exocyclic amino groups of dC and dA to form N^4-cholyl-dC and N^6-cholyl-dA, respectively (Figures 3 and 4).

To confirm chemical structures of these adducts, the deduced compounds, dC- and dA-cholamide, were synthesized as outlined in Schemes 2 and 3, respectively. Because of the difficulty of fully protecting hydroxy groups, cholic acid was applied without protection. Silyl-protected dC was reacted with cholic acid under the conditions of DCC in pyridine at a reaction temperature of 70 °C. Half the amount of dC remained intact on TLC

Scheme 2. Synthesis of N^4-Cholyl-dC

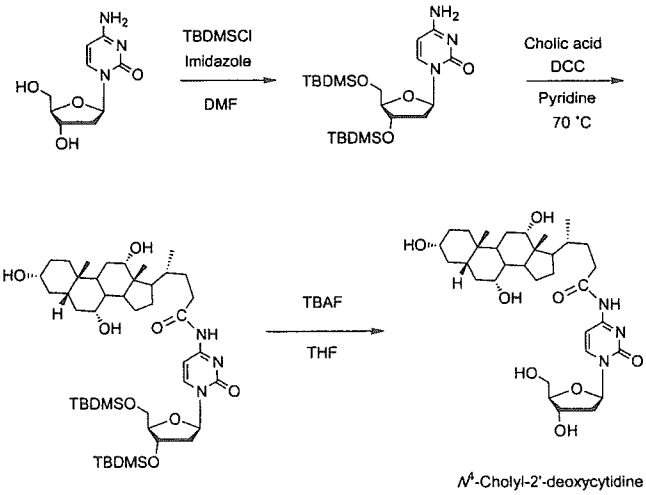

analyses after 4 h of reaction, and with a more prolonged reaction time, coupling did not proceed further. The desired product was easily separated from silyl-protected

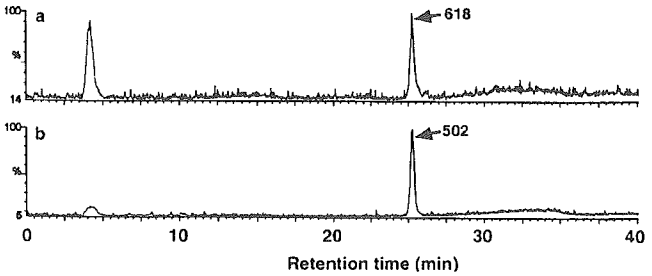

Figure 5. LC-ESI-MS chromatogram of enzymatic hydrolysates of calf thymus DNA reacted with cholyl adenylate. Cholyl adenylate (4 mg) was incubated with DNA (2 mg) at 37 °C, pH 7.0, in 100 mM phosphate buffer. DNA was then recovered from the overnight reaction mixture, followed by enzymatic hydrolysis. (a) Selected ion monitoring at *m/z* 618, which is estimated to be molecular ion of dC modified with cholic acid; (b) selected ion monitoring at *m/z* 502 derived from loss of the deoxyribose moiety from the parent dC-cholic acid adduct with a molecular ion of *m/z* 618.

Scheme 3. Synthesis of N^6-Cholyl-dA

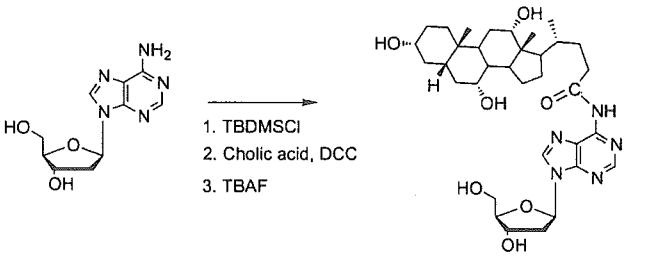

N^6-Cholyl-2'-deoxyadenosine

dC by column chromatography using silica gel. Partially purified silyl-protected dC-cholamide was then treated with 1 M TBAF in THF (Scheme 2). After column separation with ODS, the desired compound was obtained at 20% yield. In a similar manner, dA-cholamide was also obtained at a yield of 7% (Scheme 3); the lower value than for dC is probably due to the lower nucleophilicity of the amino moiety. NMR spectra of these authentic compounds showed diminishing exocyclic NH_2 peaks of dC and dA, whereas new peaks around 10.6−10.7 ppm were observed, confirming introduction of cholic acid at exocyclic amino groups to form amide groups (see Supporting Information of MS spectra of N^4-cholyl-dC and N^6-cholyl-dA). UV absorbance patterns of these synthetic compounds were the same as with reaction products of dC with cholyl adenylate and of dA with cholyl adenylate, respectively. HPLC-MS chromatograms of these compounds were also shown to be identical to those of the products obtained in cholyl adenylate reactions with dC or dA. Therefore, they were concluded to be N^4-cholyl-dC and N^6-cholyl-dA, respectively.

When calf thymus DNA incubated with cholyl adenylate was enzymatically digested and the hydrolysates were applied to LC-MS analyses, LC-MS chromatography clearly showed the presence of a peak of *m/z* 618 accompanied with *m/z* 502, as shown in Figure 5, indicating that N^4-cholyl-dC was formed (see Supporting Information for further information). The yield was around 1.6 adducts per 10^5 nucleosides calculated from the original amount of DNA. In the same reaction mixture, no peak of dA modified with cholic acid (*m/z* 642) was detected under the applied HPLC conditions with the detection limit of around 1 adduct per 10^6 nucleosides (see Supporting Information for an HPLC-UV chromatogram, UV, and full scan MS spectra of N^4-cholyl-dC obtained from the reaction of calf thymus DNA with cholyl adenylate).

Cholyl adenylate has the conjugate acid anhydride moiety arising from carboxylic acid and phosphoric acid. The reaction mechanism thus follows that of a general acid anhydride, which is initiated by the attack of nucleophiles to the carbon atom of the carbonyl group. Reaction of acid anhydride with nucleobases is well-documented for the purpose of protection of functional groups. Generally, nucleophilic substituents such as hydroxyl groups in a deoxyribose moiety and amino groups in a base moiety are targets of acid anhydride. Reactivity of cholyl adenylate with deoxynucleosides, therefore, depends on the nucleophilicity of substrates, resulting in more favorable formation of dC adducts with cholic acid and lesser amounts of the dA adduct as estimated from pK_a values of protonated forms of deoxynucleosides (pK_a = 4.3 for dC and 3.8 for dA) (*26*). Although genotoxicity with bile acids has been reported, the nature of this toxicity is not fully elucidated yet (*12*, 27). Carboxylic acid-acyl adenylates are common intermediates for CoA ester formation, and some have been detected in cells (*13*, *20*, *21*). In vivo, cholyl-CoA itself could provide *N*-cholyl derivatives. Additionally, present studies clearly showed sufficient activity to modify DNA with cholic acid via an acyl adenylate intermediate, indicating a great possible involvement of commonly known acyl adenylates to genotoxicity. The study of in vivo modification of DNA with cholic acid is now being undertaken in our laboratory.

Acknowledgment. This study was supported by a Grant-in-Aid for Cancer Research from the Ministry of Health, Labor, and Welfare, Japan.

Supporting Information Available: MS spectra of N^4-cholyl-dC and N^6-cholyl-dA and HPLC-UV chromatograms, UV spectra, and MS spectra of N^4-cholyl-dC obtained from the reaction of calf thymus DNA with cholyl adenylate. This material is available free of charge via the Internet at http://pubs.acs.org.

References

(1) Setchell, K. D. R., and Russell, D. W. (1994) In *Liver Disease in Children* (Suchy, F. J., Ed.) pp 81−104, Mosby, St. Louis, MO.
(2) Vlahcevic, Z. R., Pandak, W. M., and Stravitz, R. T. (1999) Regulation of bile acid biosynthesis. *Gastroenterol. Clin. North Am. 28*, 1−25.
(3) Chaplin, M. F. (1998) Bile acids, fibre and colon cancer: The story unfolds. *J. R. Soc. Health 118*, 53−61.
(4) Weisburger, J. H., Reddy, B. S., Barnes, W. S., and Wynder, E. L. (1983) Bile acids, but not neutral sterol, are tumor promoters in the colon in man and in rodents. *Environ. Health Perspect. 50*, 101−107.
(5) Reddy, B. S., Watanabe, K., Weisburger, J. H., and Wynder, E. L. (1977) Promoting effect of bile acids in colon carcinogenesis in germ-free and conventional F344 rats. *Cancer Res. 37*, 3238−3242.
(6) Mahmound, N. N., Dannenberg, A. J., Bilinski, R. T., Mestre, J. R., Chadburn, A., Churchill, M., Martuccii, C., and Bertagnolli, M. M. (1999) Administration of an unconjugated bile acid increases duodenal tumors in a murine model of familial adenomatous polyposis. *Carcinogenesis 20*, 299−303.
(7) Imray, C. H., Radley, S., Davis, A., Barker, G., Hendrickse, C. W., Donovan, I. A., Lawson, A. M., Baker, P. R., and Neoptolemos, J. P. (1992) Faecal unconjugated bile acids in patients with colorectal cancer or polyps. *Gut 33*, 1239−1245.
(8) Reddy, B. S., Mastromarino, A., Gustafson, C., Lipkin, M., and Wynder, E. L. (1976) Fecal bile acids and neutral sterols in patients with familial polyposis. *Cancer 38*, 1694−1698.
(9) Scates, D. K., Spigelman, A. D., Phillips, R. K., and Venitt, S. (1997) The use of ^{32}P-postlabeling in studies of the nature and

origin of DNA adducts formed by bile from patients with familial adenomatous polyposis and from normal patients. *Mutat. Res. 378*, 113−125.
(10) Hamada, K., Umemoto, A., Kajikawa, A., Seraj, M. J., and Monden, Y. (1994) In vitro formation of DNA adducts with bile acids. *Carcinogenesis 15*, 1911−1915.
(11) Shibuya, N., Nakadaira, H., Ohta, T., Nakamura, K., Hori, Y., Yamamoto, M., Saitoh, Y., and Ogoshi, K. (1997) Co-mutagenicity of glyco- and tauro-deoxycholic acids in the Ames test. *Mutat. Res. 395*, 1−7.
(12) Glinghammar, B., Inoue, H., and Rafter, J. J. (2002) Deoxycholic acid causes DNA damage in colonic cells with subsequent induction of caspases, *COX-2* promoter activity and the transcription factors NF-kB and AP-1. *Carcinogenesis 23*, 839−845.
(13) Ikegawa, S., Ishikawa, H., Oiwa, H., Nagata, M., Goto, J., Kozaki, T., Gotowda, M., and Asakawa, N. (1991) Characterization of cholyl-adenylate in rat liver microsomes by liquid chromatography/electrospray ionization-mass spectrometry. *Anal. Biochem. 266*, 125−132.
(14) Mano, N., Uchida, M., Okuyama, H., Sasaki, I., Ikegawa, S., and Goto, J. (2001) Simultaneous detection of cholyl adenylate and coenzyme A thioester utilizing liquid chromatography/electrospray ionization mass spectrometry. *Anal. Sci. 17*, 1037−1042.
(15) Goto, J., Nagata, M., Mano, N., Kobayashi, N., Ikegawa, S., and Kiyonami, R. (2001) Bile acid acyl adenylate: a possible intermediate to produce a protein-bound bile acid. *Rapid Commun. Mass Spectrom. 15*, 104−109.
(16) Mano, N., Kasuga, K., Kobayashi, N., and Goto, J. (2004) A nonenzymatic modification of the amino-terminal domain of histone H3 by bile acid acyl adenylate. *J. Biol. Chem. 279*, 55034−55041.
(17) Mihalik, S. J., Steinberg, S. J., Pei, Z., Park, J., Kim, do G., Heinzer, A. K., Dacremont, G., Wanders, R. J., Cuebas, D. A., Smith, K. D., and Watkins, P. A. (2002) Participation of two members of the very long-chain acyl-CoA synthetase family in bile acid synthesis and recycling. *J. Biol. Chem. 277*, 24771−24779.
(18) Steinberg, S. J., Mihalik, S. J., Kim, D. G., Cuebas, D. A., and Watkins, P. A. (2000) The human liver-specific homologue of very long-chain acyl-CoA synthetase is cholate:CoA ligase. *J. Biol. Chem. 275*, 15605−15608.
(19) Solaas, K., Ulvestad, A., Soreide, O., and Kase, B. F. (2000) Subcellular organization of bile acid amidation in human liver: A key issue in regulating the biosynthesis of bile salts. *J. Lipid Res. 41*, 1154−1162.
(20) DeMoss, J. A., Genuth, S. M., and Novelli, G. D. (1956) The enzymatic activation of amino acids via their acyl-adenylate derivatives. *Biochemistry 42*, 325−332.
(21) Mao, L. F., Millington, D. S., and Schulz, H. (1992) Formation of a free acyl adenylate during the activation of 2-propylpentanoic acid. Valproyl-AMP: A novel cellular metabolite of valproic acid. *J. Biol. Chem. 267*, 3143−3146.
(22) Turjman, N., and Nair, P. P. (1981) Nature of tissue-bound lithocholic acid and its implications in the role of bile acids in carcinogenesis. *Cancer Res. 41*, 3761−3763.
(23) Enya, T., Kawanishi, M., Suzuki, H., Matsui, S., and Hisamatsu, Y. (1998) An unusual DNA adduct derived from the powerfully mutagenic environmental contaminant 3-nitrobenzanthrone. *Chem. Res. Toxicol. 11*, 1460−1467.
(24) Ogilvie, K. K. (1973) The *tert*-butyldimethylsilyl group as a protecting group in deoxynucleosides. *Can. J. Chem. 51*, 3799−3807.
(25) Acedo, M., Fàbrega, C., Aviño, A., Goodman, M., Fagan, P., Wemmer, D., and Eritja, R. (1994) A simple method for N-15 labeling of exocyclic amino groups in synthetic oligodeoxynucleotides. *Nucleic Acids Res. 22*, 2982−2989.
(26) Sekine, M., Ohkubo, A., and Seio, K. (2003) Proton-block strategy for the synthesis of oligodeoxynucleotides without base protection, capping reaction, and P−N bond cleavage reaction. *J. Org. Chem. 68*, 5478−5492.
(27) Scates, D. K., Spigelman, A. D., and Venitt, S. (1994) Bile acids do not form adducts when incubated with DNA in vitro. *Carcinogenesis 15*, 2945−2948.

TX050159V

Carcinogenesis vol.27 no.3 pp.619–630, 2006
doi:10.1093/carcin/bgi241
Advance Access publication October 11, 2005

An animal model for the rapid induction of tongue neoplasms in human c-Ha-*ras* proto-oncogene transgenic rats by 4-nitroquinoline 1-oxide: its potential use for preclinical chemoprevention studies

Rikako Suzuki[1,2], Hiroyuki Kohno[1], Masumi Suzui[3], Naoki Yoshimi[3], Hiroyuki Tsuda[4], Keiji Wakabayashi[5] and Takuji Tanaka[1,*]

[1]Department of Oncologic Pathology, Kanazawa Medical University, 1-1 Daigaku, Uchinada, Ishikawa 920-0293, Japan, [2]Japan Society for the Promotion of Science, 6 Ichiban-cho, Chiyoda-ku, Tokyo 102-8471, Japan, [3]Department of Tumor Pathology, University of the Ryukyus Faculty of Medicine, 207 Uehara Nishihara-cho, Okinawa 903-0215, Japan, [4]Department of Molecular Toxicology, Graduate School of Medical Sciences, Nagoya City University, 1 Kawasumi, Mizuho-cho, Mizuho-ku, Nagoya 467-8601, Japan and [5]Cancer Prevention Basic Research Project, National Cancer Research Institute, 5-1-1 Tsukiji, Chuo-ku, Tokyo 104-0045, Japan

*To whom correspondence should be addressed. Tel: +81 76 286 2211 (ext. 3611); Fax: +81 76 286 6926;
E-mail: takutt@kanazawa-med.ac.jp

Oral squamous cell carcinoma is one of the most common human neoplasms, and prevention of this malignancy requires a better understanding of its carcinogenesis process. To this end, we tried to establish an animal model using the human c-Ha-*ras* proto-oncogene-carrying transgenic (Tg) rats and the carcinogen 4-nitroquinoline 1-oxide (4-NQO). 4-NQO (20 p.p.m.) was administered to Tg and non-Tg rats for 8 weeks in their drinking water, and then the occurrence of tongue carcinogenesis was compared during the experimental period of 22 weeks. In addition, we determined the DNA ploidy in tongue lesions and examined the immunohistochemical expression of five biomarkers such as cyclin D1, glutathione *S*-transferase placental form, cyclooxygenase (COX)-2, inducible nitric oxide synthase (iNOS) and β-catenin. Next, the cancer chemopreventive effects of nimesulide, pioglitazone and a synthetic geranylated derivative, which have been reported to be inhibitors of tongue carcinogenesis, were examined in Tg rats treated with 4-NQO. Either during or after treatment with 4-NQO in the drinking water, tongue dysplasia and tumors were observed on the tongues of both Tg and non-Tg rats, with a greater incidence and multiplicity in Tg rats. Histopathologically, squamous cell dysplasia, papilloma and carcinoma with or without invasion were present in the tongue. Immunohistochemistry revealed that expression levels against five biomarkers increase with disease progression, and the changes correlated with those of the DNA ploidy pattern. Interestingly, a strong expression of COX-2, iNOS and β-catenin was observed on the invasive front of squamous cell carcinomas. A subsequent chemoprevention study using Tg rats showed that the chemicals tested suppressed the occurrence of tongue carcinomas when they were administered after 4-NQO-exposure. These results may thus indicate that our 4-NQO-induced Tg rat tongue carcinogenesis model simulates many aspects of human oral carcinogenesis and it can be applied for an analysis of oral cancer development while also helping to identify potentially effective cancer chemopreventive agents against oral cancer.

Abbreviations: CDK, cyclin-dependent kinase; COX, cyclooxygenase; DMBA, 7,12-dimethylbenz(*a*)anthracene; EGMP, ethyl 3-(4′-geranyloxy-3′-methoxyphenyl)-2-propenoate; GST-P, glutathione *S*-transferase placental form; H&E, hematoxylin and eosin; iNOS, inducible nitric synthase; NO, Nitric oxide; 4-NQO, 4-nitroquinoline 1-oxide; PPAR, peroxisome proliferator-activated receptor; SCC, squamous cell carcinoma; Tg rats, Human c-Ha-ras proto-oncogene carrying transgenic rats.

Introduction

Oral cancer, mostly squamous cell carcinoma (SCC), is considered to be one of the most common neoplasms in the world with nearly 390 000 new cases per year (1). This malignancy is particularly common in such developing countries as India, Sri Lanka, Vietnam, the Philippines and Brazil, where it constitutes up to 25% of all types of cancers (2). Recently, the oral cancer incidence and mortality rates have been increasing in the USA, Japan, Germany and Scotland, especially among young males (3–5). In addition, many patients tend to develop secondary primary tumors even if the primary tumors can be treated (6). This suggests the occurrence of a multi-focal tumor development, called 'field cancerization' (7). As a result, the development of cancer chemoprevention is an important strategy for fighting this malignancy (8–10), and an animal model for preclinical studies is warranted to clarify how best to control this epithelial malignancy.

Several animal models for oral carcinoma development were utilized, including hamster, rats and mouse models. The most commonly used model is 7,12-dimethylbenz(*a*)anthracene (DMBA)-induced hamster cheek pouch carcinogenesis model (11) and ~60% of all SCC have a mutation in codon 61 of Ha-*ras* gene (12). Treatment by the administration of 4-nitroquinoline 1-oxide (4-NQO) in drinking water can induce tumors in oral cavities in rats (13) and mice (14). Oral SCCs induced by 4-NQO in rats, which shows morphological and histopathological similarities to those of human tumors, have been extensively used to investigate and test a wide variety of synthetic and natural agents for chemopreventive potential (8).

Mutations in the three *ras* genes and *p53* gene are observed in human cancers, including oral cancer (15–18). Activating mutations in K-*ras* and H-*ras* have been reported in human oral SCCs , primarily in those caused by exposure to carcinogens that are present in betel quid (19). In addition, *ras* activation involves murine oral squamous carcinogenesis (20,21), although some exceptions have been reported (22). The development of oral cancer appears to be a continuum, a progression from the early stage of oral lesions to SCC and metastasis. The results of animal model studies could thus translate directly or indirectly to clinical patients' care initiatives or at least allow targeted studies that make the best use of human clinical trials. 4-NQO-induced rat tongue carcinogenesis is such a model. In addition, genetically modified animal models are also useful